

NISTIR 4633

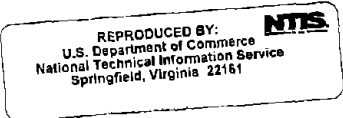
ULTIMATE STRENGTH OF MASONRY SHEAR WALLS: PREDICTIONS VS TEST RESULTS

S. G. Fattal
D. R. Todd

October 1991



U.S. Department of Commerce
Robert A. Mosbacher, *Secretary*
National Institute of Standards and Technology
John W. Lyons, *Director*
Building and Fire Research Laboratory
Gaithersburg, MD 20899





NIST-114A (REV. 3-90)	U.S. DEPARTMENT OF COMMERCE NATIONAL INSTITUTE OF STANDARDS AND TECHNOLOGY	1. PUBLICATION OR REPORT NUMBER NISTIR 4633								
BIBLIOGRAPHIC DATA SHEET		2. PERFORMING ORGANIZATION REPORT NUMBER								
4. TITLE AND SUBTITLE Ultimate Strength of Masonry Shear Walls: Predictions Vs Test Results		3. PUBLICATION DATE OCTOBER 1991								
5. AUTHOR(S) S. G. Fattal D. R. Todd										
6. PERFORMING ORGANIZATION (IF JOINT OR OTHER THAN NIST, SEE INSTRUCTIONS) U.S. DEPARTMENT OF COMMERCE NATIONAL INSTITUTE OF STANDARDS AND TECHNOLOGY GAITHERSBURG, MD 20899	7. CONTRACT/GRANT NUMBER									
9. SPONSORING ORGANIZATION NAME AND COMPLETE ADDRESS (STREET, CITY, STATE, ZIP)		8. TYPE OF REPORT AND PERIOD COVERED								
10. SUPPLEMENTARY NOTES <p style="text-align: right;">NIST CATEGORY * 140</p>										
11. ABSTRACT (A 200-WORD OR LESS FACTUAL SUMMARY OF MOST SIGNIFICANT INFORMATION. IF DOCUMENT INCLUDES A SIGNIFICANT BIBLIOGRAPHY OR LITERATURE SURVEY, MENTION IT HERE.) <p>→ This study compares the ability of four different equations to predict the ultimate shear stress in masonry walls failing in shear. Experimental data on full-grouted reinforced shear walls from four different sources are compared with the predictions from the four equations. Wall characteristics from 65 test specimens were used as input to the four predictive equations. The ultimate strength predictions were then compared to the actual measured strength of the 65 test walls.</p> <p>Two of the equations (the existing UBC equation for shear strength of masonry walls and the Architectural Institute of Japan's equation for predicting the shear strength of reinforced concrete shear walls) were found to be inadequate for the prediction of ultimate shear strength of masonry walls. An equation proposed by Shing et al. was found to predict shear strength well for only limited ranges of variables, primarily because excessive weight is given to the contributions of horizontal reinforcement to strength. An equation proposed by Matsumura was found to be the best predictor of the four equations examined, but it lacks the consistency needed to use it as a basis for design. ←</p> <p>The conclusions drawn from the present study indicate the possibility of developing reliable predictive formulations using both rational analysis and an empirical approach.</p>										
12. KEY WORDS (6 TO 12 ENTRIES; ALPHABETICAL ORDER; CAPITALIZE ONLY PROPER NAMES; AND SEPARATE KEY WORDS BY SEMICOLONS) Masonry; predicted strength; reinforced walls; shear strength; shear walls; test strength; ultimate load										
13. AVAILABILITY <table border="1" style="width: 100%; border-collapse: collapse;"> <tr> <td style="width: 20px; text-align: center;"><input checked="" type="checkbox"/></td> <td>UNLIMITED</td> </tr> <tr> <td style="text-align: center;"><input type="checkbox"/></td> <td>FOR OFFICIAL DISTRIBUTION. DO NOT RELEASE TO NATIONAL TECHNICAL INFORMATION SERVICE (NTIS).</td> </tr> <tr> <td style="text-align: center;"><input type="checkbox"/></td> <td>ORDER FROM SUPERINTENDENT OF DOCUMENTS, U.S. GOVERNMENT PRINTING OFFICE, WASHINGTON, DC 20402.</td> </tr> <tr> <td style="text-align: center;"><input checked="" type="checkbox"/></td> <td>ORDER FROM NATIONAL TECHNICAL INFORMATION SERVICE (NTIS), SPRINGFIELD, VA 22161.</td> </tr> </table>	<input checked="" type="checkbox"/>	UNLIMITED	<input type="checkbox"/>	FOR OFFICIAL DISTRIBUTION. DO NOT RELEASE TO NATIONAL TECHNICAL INFORMATION SERVICE (NTIS).	<input type="checkbox"/>	ORDER FROM SUPERINTENDENT OF DOCUMENTS, U.S. GOVERNMENT PRINTING OFFICE, WASHINGTON, DC 20402.	<input checked="" type="checkbox"/>	ORDER FROM NATIONAL TECHNICAL INFORMATION SERVICE (NTIS), SPRINGFIELD, VA 22161.	14. NUMBER OF PRINTED PAGES 46 15. PRICE A03	
<input checked="" type="checkbox"/>	UNLIMITED									
<input type="checkbox"/>	FOR OFFICIAL DISTRIBUTION. DO NOT RELEASE TO NATIONAL TECHNICAL INFORMATION SERVICE (NTIS).									
<input type="checkbox"/>	ORDER FROM SUPERINTENDENT OF DOCUMENTS, U.S. GOVERNMENT PRINTING OFFICE, WASHINGTON, DC 20402.									
<input checked="" type="checkbox"/>	ORDER FROM NATIONAL TECHNICAL INFORMATION SERVICE (NTIS), SPRINGFIELD, VA 22161.									

CONTENTS

	Page
ABSTRACT	iii
PREFACE	iv
1. INTRODUCTION	1
2. OBJECTIVE	2
3. SCOPE	2
3.1 Experimental Data Sets	2
3.2 Predictive Equations	6
3.3 Notation	8
4. METHODOLOGY	10
5. RESULTS AND ANALYSIS	17
5.1 Results	17
5.2 Analysis of Data	20
5.3 Analysis of Strength Prediction	26
6. CONCLUSIONS	31
7. RECOMMENDATIONS	31
8. REFERENCES	31
APPENDIX A - Tables	33
APPENDIX B - Derivations	38



ABSTRACT

This study compares the ability of four different equations to predict the ultimate shear stress in masonry walls failing in shear. Experimental data on fully-grouted reinforced shear walls from four different sources are compared with the predictions from the four equations. Wall characteristics from 62 test specimens were used as input to the four predictive equations. The ultimate strength predictions were then compared to the actual measured strength of the 62 test walls.

Two of the equations (the existing Uniform Building Code equation for shear strength of masonry walls and the Architectural Institute of Japan's equation for predicting the shear strength of reinforced concrete shear walls) were found to be inadequate for the prediction of ultimate shear strength of masonry walls. An equation proposed by Shing et al. was found to predict shear strength well for only limited ranges of variables, primarily because excessive weight is given to the contributions of horizontal reinforcement to strength. An equation proposed by Matsumura was found to be the best predictor of the four equations examined, but it lacks the consistency needed to use it as a basis for design.

The conclusions drawn from the present study indicate the possibility of developing reliable predictive formulations using both rational analysis and an empirical approach.

Key Words: Masonry; predicted strength; reinforced walls; shear strength; shear walls; test strength; ultimate load

PREFACE

SI units are used in this report. However, U.S. Customary units are also specified to conform with current practices of the masonry industry in the United States. Codes and standards, construction specifications and tolerances, and nominal and actual sizes of standard masonry units manufactured in the United States are all currently measured in U.S. Customary Units. This system of measure was therefore used as a supplement to aid the masonry industry and standards organizations in utilizing the results of this investigation.

1. INTRODUCTION

The last decade has seen the rapid evolution of reinforced masonry as an engineered construction material, increasingly allowing masonry buildings to be considered as viable alternatives to concrete or steel structures. By stimulating competition and reducing building costs, improved masonry design enhances U.S. construction productivity in both domestic and international markets. Increased safety for occupants, especially during earthquakes, is another benefit the nation reaps from the improved procedures being developed for engineered masonry buildings. Federally funded research has contributed significantly to the rapid progress that has been made in recent years.

As part of the ongoing effort to improve masonry technology and to make masonry design and analysis methodologies comparable to those of concrete and steel, limit state design procedures are being developed. Major progress towards understanding the ultimate behavior of masonry walls has been made, in large part through research conducted under the auspices of the Joint U.S.-Japan Technical Coordinating Committee on Masonry Research (better known as JTCCMAR). JTCCMAR coordinates masonry research on material behavior and seismic response analysis and design in the United States and Japan. The U.S. research is coordinated by the Technical Coordinating Committee for Masonry Research (TCCMAR).

Since its inception in 1984, a substantial amount of TCCMAR research has been sponsored by the National Science Foundation (NSF) under the National Earthquake Hazards Reduction Program (NEHRP), which was established in accordance with the National Earthquake Hazards Reduction Act passed by the U.S. Congress in 1977. That legislation assigned the National Bureau of Standards (now known as the National Institute of Standards and Technology or NIST) the mission to assist in the development of improved design procedures for buildings subject to earthquakes. The NIST Masonry Research Program is coordinated with the JTCCMAR programs.

A recent NIST report titled "Review of Research Literature on Masonry Shear Walls" [1] reviews the existing literature on experimental research on masonry shear walls conducted during the past 15 years. The report recommends that the accuracy and reliability of proposed formulations for predicting masonry shear wall strength under lateral and gravity loads be assessed. The present study implements this recommendation in part, through comparisons of the experimentally observed shear strengths of fully-grouted walls with predictions according to four different equations for evaluating shear strength.

A detailed description of the predictive equations and the data sets used in this study are included in Section 3. The methodology used in the comparison is

described in Section 4. Section 5 presents and analyzes the results of the comparative study. Conclusions drawn from the study and possible topics for additional investigations are described in Sections 6 and 7.

2. OBJECTIVE

The objective of this study was to evaluate the accuracy of empirical equations in predicting in-plane shear strength of fully grouted concrete and clay masonry walls. Accuracy was assessed by comparing predicted strengths to actual tested strengths. Four equations were checked against four sets of experimental data from independent research sources. Two of the equations assessed here are part of existing code provisions. The other two empirical equations are proposed formulas which have been developed using experimental data. These experimental data sets were among the four sets used in this study to evaluate the accuracy of predicted strength. By cross-checking an equation from one source against data from another source and against the much larger combined data set, the accuracy and consistency of the equations were assessed, within the ranges of parameters used in the experiments.

3. SCOPE

The report titled "Review of Technical Literature on Masonry Shear Walls" [1] guided the selection of the predictive equations and experimental data sets to be used. Results from some 700 independent tests, along with accompanying documentation regarding the geometric and material properties of the test specimens, methods of testing, and variation of design parameters, are included in that report. Test results of laterally loaded specimens of fully-grouted reinforced masonry were selected for this study. Partially-grouted masonry walls were not included in the present study.

3.1 Experimental Data Sets

The data sets included in this study were limited to results from fully-grouted reinforced masonry walls which were subjected to reverse cyclic lateral loads until failure in the shear mode occurred. Three data sets were obtained from tests in which the top and bottom surfaces of the specimens were rotationally fixed. One data set, obtained from tests conducted by Shing et al, used specimens which were rotationally free at the top (i.e. cantilever walls). Both clay and concrete unit masonry walls were represented in the tests. The scope of the experiments and the range of test variables were other factors taken into consideration in the selection of the data. The data sets selected for this study were assembled from the following experimental programs:

- 1) tests conducted by Shing et al. at the University of Colorado under the U.S.-Japan Joint Technical Committee on Masonry Research (JTCCMAR) program [2,3],
- 2) tests conducted by Matsumura at Kanagawa University in Japan [4],
- 3) tests conducted by Okamoto et.al. at Japan's Building Research Institute, Ministry of Construction, in connection with the JTCCMAR program [5], and
- 4) masonry research conducted by Sveinsson et al. at the University of California at Berkeley [6].

Each of the experimental studies used displacement-controlled tests consisting of multiple cycles of reversed loadings. Predefined load-displacement histories characterized by increasing amplitudes to failure were used. The common loading procedure and the use of similar loading rates in each of the four studies produced comparable tests. The load-displacement histories are described in detail in the cited references.

Ultimate shear strength was defined as the average of the two peak shear forces attained in the two opposite directions of cyclic loading. Shear strength was calculated using gross area based on actual dimensions. Data from specimens that were reported to have failed in bending were eliminated. The final data set consisted of 62 separate tests. The data subsets finally selected from the studies listed above are identified in the text by the letters S, M, O and B, respectively.

Relevant properties of the specimens are listed in Table 1. Definitions of symbols used in column headings of the table are included in section 3.3. The four groups are identified by the suffix (S, M, O, or B) appended to the specimen identification tag in the second column. There are 10 S, 18 M, 9 O, and 25 B specimens. Specimens 21-S, 22-S, WSR2-M, WSR4-M, WSR5-M, WSR6-M, WSR1-O, WSR4-O, WSR7-O, and the nine B specimens designated by BR are single-wythe walls constructed with hollow brick units. The four B specimens designated by DBR are two-wythe grouted walls built with solid brick units. Specimen WSRC-O is a reinforced concrete shear wall which was included primarily because one of the empirical formulas examined in this study was developed for reinforced concrete shear walls. Its inclusion does not significantly affect the evaluations of accuracy performed in this study. The

TABLE 1. PROPERTIES OF SPECIMENS

TEST NUMBER	SPECIMEN LABEL	h mm	L mm	t mm	d mm	sh mm	r	rd	f _m MPa	f _{yh} MPa
1	3-S	1829	1829	143	1727	406	1.00	1.06	20.87	385.84
2	4-S	1829	1829	143	1727	406	1.00	1.06	17.91	385.84
3	5-S	1829	1829	143	1727	406	1.00	1.06	17.91	385.84
4	7-S	1829	1829	143	1727	406	1.00	1.06	20.87	385.84
5	9-S	1829	1829	143	1727	406	1.00	1.06	20.87	385.84
6	13-S	1829	1829	143	1727	406	1.00	1.06	22.74	461.63
7	14-S	1829	1829	143	1727	406	1.00	1.06	22.74	385.84
8	16-S	1829	1829	143	1727	406	1.00	1.06	17.23	461.63
9	21-S	1829	1829	137	1727	406	1.00	1.06	26.18	385.84
10	22-S	1829	1829	137	1727	406	1.00	1.06	26.18	385.84
11	KW4-1-M	1800	1690	150	1500	400	1.13	1.20	21.80	385.00
12	KW3-1-M	1800	1190	150	1100	400	1.51	1.64	21.80	385.00
13	KW3S-1-	1800	1190	150	1100	400	1.51	1.64	21.80	385.00
14	KW2-1-M	1800	790	150	700	400	2.28	2.57	21.80	385.00
15	WS2-M	1800	1190	190	1095	400	1.51	1.64	22.30	385.00
16	WS4-M	1800	1190	190	1095	400	1.51	1.64	22.30	385.00
17	WS5-M	1800	1190	190	1095	400	1.51	1.64	22.30	385.00
18	WS9-M	1800	1190	190	1095	400	1.51	1.64	22.30	385.00
19	WS10-M	1800	1190	190	1095	400	1.51	1.64	22.30	385.00
20	WS9-2-M	1800	1190	190	1095	400	1.51	1.64	29.00	385.00
21	WSB21-M	1800	1190	190	1095	400	1.51	1.64	26.10	385.00
22	WSB22-M	1800	1190	190	1095	400	1.51	1.64	27.40	385.00
23	WSB3-M	1800	1190	190	1095	400	1.51	1.64	26.40	385.00
24	WSB4-M	1800	1190	190	1095	400	1.51	1.64	31.40	385.00
25	WSR2-M	1700	1110	190	1005	378	1.53	1.69	28.60	385.00
26	WSR4-M	1700	1110	190	1005	378	1.53	1.69	28.60	385.00
27	WSR5-M	1700	1110	190	1005	378	1.53	1.69	28.60	385.00
28	WSR8-M	1700	1110	190	1005	378	1.53	1.69	28.60	385.00
29	WS1-O	1800	2000	190	1905	400	0.90	0.94	17.91	354.44
30	WS4-O	1800	1200	190	1105	400	1.50	1.63	22.81	354.44
31	WS7-O	1800	800	190	705	400	2.25	2.55	17.91	354.44
32	WSN1-O	1800	1200	190	1105	400	1.50	1.63	22.81	354.44
33	WSN2-O	1800	1200	190	1105	400	1.50	1.63	22.81	354.44
34	WSR1-O	1800	2000	190	1905	400	0.90	0.94	26.73	354.44
35	WSR4-O	1800	1200	190	1105	400	1.50	1.63	25.16	354.44
36	WSR7-O	1800	800	190	705	400	2.25	2.55	21.35	354.44
37	WSRC-O	1800	1200	190	1105	400	1.50	1.63	26.73	354.44
38	CB13-B	1422	1219	194	1143	284	1.17	1.24	23.14	406.51
39	CB15-B	1422	1219	194	1143	284	1.17	1.24	23.14	406.51
40	CB17-B	1422	1219	143	1143	284	1.17	1.24	15.83	437.52
41	CB18-B	1422	1219	143	1143	284	1.17	1.24	15.83	437.52
42	CB20-B	1422	1219	143	1143	474	1.17	1.24	15.13	437.52
43	CB21-B	1422	1219	143	1143	474	1.17	1.24	15.13	437.52
44	CB23-B	1422	1219	143	1143	203	1.17	1.24	15.13	437.52
45	CB24-B	1422	1219	143	1143	399	1.17	1.24	15.13	437.52
46	CB25-B	1422	1219	143	1143	474	1.17	1.24	15.13	437.52
47	CB26-B	1422	1219	143	1143	474	1.17	1.24	15.13	437.52
48	BR19-B	1422	1219	143	1143	474	1.17	1.24	20.11	437.52
49	BR20-B	1422	1219	143	1143	237	1.17	1.24	20.11	437.52
50	BR21-B	1422	1219	143	1143	474	1.17	1.24	20.11	437.52
51	BR22-B	1422	1219	143	1143	237	1.17	1.24	20.11	437.52
52	BR23-B	1422	1219	143	1143	474	1.17	1.24	20.11	437.52
53	BR24-B	1422	1219	143	1143	237	1.17	1.24	20.11	437.52
54	BR25-B	1422	1219	143	1143	474	1.17	1.24	20.11	437.52
55	BR26-B	1422	1219	143	1143	237	1.17	1.24	20.11	437.52
56	BR27-B	1422	1219	143	1143	284	1.17	1.24	20.11	409.96
57	BR28-B	1422	1219	143	1143	129	1.17	1.24	20.11	416.85
58	BR30-B	1422	1219	143	1143	203	1.17	1.24	27.62	437.52
59	DBR8S-B	1422	1219	254	1143	711	1.17	1.24	17.11	406.51
60	DBR9-B	1422	1219	254	1143	237	1.17	1.24	17.11	465.08
61	DBR10-B	1422	1219	254	1143	711	1.17	1.24	17.11	406.51
62	DBR12-B	1422	1219	254	1143	356	1.17	1.24	17.11	398.24

TABLE 1. CONT'D PROPERTIES OF SPECIMENS

TEST NUMBER	SPECIMEN LABEL	f _{ye} MPa	f _{yi} MPa	f _{vy} MPa	ph	p _{ve}	p _{vi}	p _v	SIGMA _O (MPa)	ALPHA
1	3-S	496.08	496.08	496.08	0.00122	0.00148	0.00667	0.00741	1.86	1
2	4-S	496.08	496.08	496.08	0.00122	0.00148	0.00667	0.00741	0.00	1
3	5-S	496.08	496.08	496.08	0.00122	0.00148	0.00667	0.00741	0.69	1
4	7-S	496.08	496.08	496.08	0.00122	0.00148	0.00667	0.00741	0.69	1
5	9-S	440.96	440.96	440.96	0.00122	0.00077	0.00344	0.00383	1.86	1
6	13-S	447.85	447.85	447.85	0.00222	0.00109	0.00489	0.00543	1.86	1
7	14-S	447.85	447.85	447.85	0.00122	0.00109	0.00489	0.00543	1.86	1
8	16-S	496.08	496.08	496.08	0.00222	0.00148	0.00667	0.00741	1.86	1
9	21-S	447.85	447.85	447.85	0.00128	0.00114	0.00512	0.00568	1.93	1
10	22-S	447.85	447.85	447.85	0.00128	0.00114	0.00512	0.00568	0.69	1
11	KW4-1-M	385.00	385.00	385.00	0.00118	0.00426	0.00134	0.00943	0.49	0.5
12	KW3-1-M	385.00	385.00	385.00	0.00118	0.00434	0.00140	0.00946	0.49	0.5
13	KW3S-1-	385.00	385.00	385.00	0.00118	0.00434	0.00140	0.00946	0.49	0.5
14	KW2-1-M	385.00	385.00	385.00	0.00118	0.00541	0.00155	0.01148	0.49	0.5
15	WS2-M	385.00	385.00	385.00	0.00000	0.00254	0.00111	0.00571	1.96	0.5
16	WS4-M	385.00	385.00	385.00	0.00167	0.00254	0.00111	0.00571	1.96	0.5
17	WS5-M	385.00	385.00	385.00	0.00334	0.00254	0.00111	0.00571	1.96	0.5
18	WS9-M	385.00	385.00	385.00	0.00334	0.00448	0.00111	0.00959	1.96	0.5
19	WS10-M	385.00	385.00	385.00	0.00668	0.00448	0.00111	0.00959	1.96	0.5
20	WS9-2-M	385.00	385.00	385.00	0.00334	0.00448	0.00111	0.00959	1.96	0.5
21	WSB21-M	385.00	385.00	385.00	0.00334	0.00448	0.00111	0.00959	1.96	0.5
22	WSB22-M	385.00	385.00	385.00	0.00400	0.00448	0.00111	0.00959	1.96	0.5
23	WSB3-M	385.00	385.00	385.00	0.00353	0.00473	0.00117	0.01013	1.96	0.5
24	WSB4-M	385.00	385.00	385.00	0.00334	0.00448	0.00111	0.00959	1.96	0.5
25	WSR2-M	385.00	385.00	385.00	0.00000	0.00272	0.00121	0.00612	1.96	0.5
26	WSR4-M	385.00	385.00	385.00	0.00167	0.00272	0.00121	0.00612	1.96	0.5
27	WSR5-M	385.00	385.00	385.00	0.00334	0.00272	0.00121	0.00612	1.96	0.5
28	WSR6-M	385.00	385.00	385.00	0.00668	0.00272	0.00121	0.00612	1.96	0.5
29	WS1-O	386.55	371.18	378.86	0.00167	0.00149	0.00292	0.00509	0.00	0.5
30	WS4-O	386.55	371.18	378.86	0.00167	0.00249	0.00316	0.00674	1.96	0.5
31	WS7-O	386.55	371.18	378.86	0.00167	0.00374	0.00351	0.00879	0.00	0.5
32	WSN1-O	386.55	371.18	378.86	0.00167	0.00249	0.00316	0.00674	3.92	0.5
33	WSN2-O	386.55	371.18	378.86	0.00167	0.00249	0.00316	0.00674	5.87	0.5
34	WSR1-O	386.55	383.05	374.80	0.00167	0.00149	0.00292	0.00509	0.00	0.5
35	WSR4-O	386.55	371.18	378.86	0.00167	0.00249	0.00316	0.00674	0.00	0.5
36	WSR7-O	386.55	371.18	378.86	0.00167	0.00374	0.00351	0.00879	0.00	0.5
37	WSRC-O	386.55	371.18	378.86	0.00167	0.00249	0.00316	0.00674	2.15	0.5
38	CB13-B	465.08	465.08	465.08	0.00281	0.00085	0.00000	0.00169	1.88	0.5
39	CB15-B	465.08	465.08	465.08	0.00281	0.00085	0.00000	0.00169	3.01	0.5
40	CB17-B	390.66	390.66	390.66	0.00394	0.00222	0.00000	0.00444	2.76	0.5
41	CB18-B	409.96	409.96	409.96	0.00394	0.00074	0.00423	0.00444	2.76	0.5
42	CB20-B	390.66	390.66	390.66	0.00197	0.00222	0.00000	0.00444	2.76	0.5
43	CB21-B	409.96	409.96	409.96	0.00197	0.00074	0.00423	0.00444	2.76	0.5
44	CB23-B	390.66	390.66	390.66	0.00075	0.00222	0.00000	0.00444	2.76	0.5
45	CB24-B	390.66	390.66	390.66	0.00272	0.00222	0.00000	0.00444	2.76	0.5
46	CB25-B	390.66	390.66	390.66	0.00197	0.00222	0.00000	0.00444	1.74	0.5
47	CB26-B	390.66	390.66	390.66	0.00197	0.00222	0.00000	0.00444	2.76	0.5
48	BR19-B	390.66	390.66	390.66	0.00197	0.00222	0.00000	0.00444	2.76	0.5
49	BR20-B	390.66	390.66	390.66	0.00492	0.00222	0.00000	0.00444	2.76	0.5
50	BR21-B	390.66	390.66	390.66	0.00197	0.00222	0.00394	0.00674	2.76	0.5
51	BR22-B	437.52	437.52	437.52	0.00492	0.00115	0.00394	0.00459	2.76	0.5
52	BR23-B	409.96	409.96	409.96	0.00197	0.00074	0.00423	0.00444	2.76	0.5
53	BR24-B	409.96	409.96	409.96	0.00492	0.00074	0.00423	0.00444	2.76	0.5
54	BR25-B	390.66	390.66	390.66	0.00197	0.00222	0.00000	0.00148	2.76	0.5
55	BR26-B	390.66	390.66	390.66	0.00492	0.00222	0.00000	0.00444	2.76	0.5
56	BR27-B	390.66	390.66	390.66	0.00254	0.00222	0.00000	0.00444	2.76	0.5
57	BR28-B	409.96	409.96	409.96	0.00835	0.00222	0.00000	0.00444	2.76	0.5
58	BR30-B	390.66	390.66	390.66	0.00100	0.00222	0.00000	0.00444	2.76	0.5
59	DBR8S-B	465.08	465.08	465.08	0.00055	0.00065	0.00000	0.00129	1.52	0.5
60	DBR9-B	465.08	465.08	465.08	0.00277	0.00065	0.00000	0.00129	2.29	0.5
61	DBR10-B	465.08	465.08	465.08	0.00055	0.00065	0.00000	0.00129	2.29	0.5
62	DBR12-B	465.08	465.08	465.08	0.00059	0.00065	0.00000	0.00129	2.29	0.5

remaining specimens are single-wythe walls built with hollow concrete block units.

Subsequent columns of Table 1 specify the geometric and material properties of the specimens, reinforcement ratios, and axial loads. The tabulated compressive strengths of masonry were obtained by prism tests. Matsumura and Shing et al used three-course prisms. Sveinsson et al. used three-course prisms with h/t ratios of 2, and six course prisms with h/t ratios of 4. The average of the results obtained from the two types of prisms was used as the value of compressive strength for the Sveinsson et al. specimens. Okamoto et al did not report the type of prism used. All researchers used tension tests to determine the yield strengths of the reinforcing steel. The U.S. Customary Units of the data presented by Shing et al and Sveinsson et al, as well as the Metric Units of data presented by Okamoto et al, were converted to SI units. The final column in Table 1 gives the experimentally-determined ultimate shear strength of the specimens. Table A1 in Appendix A duplicates Table 1 using U.S. Customary Units.

3.2 Predictive Equations

Four equations for the prediction of the ultimate shear strength of fully-grouted reinforced masonry shear walls in which shear is the characteristic mode of failure were selected for study. Two of the equations are of Japanese origin (equations M and J below), and two are of American origin (S and U). Two of the equations (U and J) are currently prescribed by codes and two (S and M) are proposed. There are other proposed formulations which use different functional forms for the effect of various parameters on strength than those examined in this study. For example, equations derived by Blondet et al [9] and Leiva [10] show good correlation with test results from University of California at Berkeley and abroad. These equations deserve further verification against a more diverse experimental data base such as used in this study. The original formats of each of the four equations were modified by introducing a common notation and consistent units. The equations shown below are in SI units. Appendix B describes the conversion of the original forms of the predictive equations into the common format and consistent units used in this report. The definitions of the symbols used in the transformed equations and in the rest of this document are given in section 3.3.

The equations selected include:

- 1) two related equations proposed by Shing et al which were developed from the data of experiments performed by Shing et al and reported in references [2] and [3] (these two equations are

combined into one comprehensive equation for the purposes of this study),

- 2) a proposed equation developed by Matsumura based on his and other experimental data and reported in reference [4],
- 3) an equation prescribed by the Architectural Institute of Japan for predicting the shear strength of concrete shear walls [5]; the data developed by Okamoto et al, as reported in [5], was used by the same authors to examine the ability of this equation to predict the shear strength of masonry walls, and,
- 4) the equation from the 1988 edition of the Uniform Building Code [7] currently in use for predicting the nominal (ultimate) shear strength of masonry walls as part of the strength design provisions for masonry.

The transformed versions of the above equations will be referred to throughout this paper as S, M, J, and U, respectively. The standard form used in the transformed equations is:

$$v_u = v_m + v_s + v_a$$

in which the term v_m represents the contribution to shear strength provided by the masonry and vertical steel, v_s represents the contribution of the horizontal steel, and v_a represents the contribution of the axial load. The transformed versions of the four equations are:

Equation S:

$$v_u = (0.0217 \rho_v f_{yv} + 0.166) \sqrt{f'_m} + \left(\frac{L - 2d'}{s_h} - 1 \right) \frac{s_h}{L} \rho_h f_{yh} + (0.0217 \sigma_o) \sqrt{f'_m}$$

Equation M:

$$v_u = \left[\left(\frac{0.76}{r_d + 0.7} + 0.012 \right) (4.04 \rho_{ve}) \sqrt{f'_m} \right] \frac{d}{L} + \left[0.01575 (\rho_h f_{yh})^{\frac{1}{2}} \sqrt{f'_m} \right] \frac{\delta d}{L} + (0.175 \sigma_o) \frac{d}{L}$$

Equation J:

$$\begin{aligned}
 v_u &= [4.64 \rho_{ve}^{0.23} (0.01 f'_m + 0.176) \left(\frac{1}{r_c + 0.12} \right)] \frac{d}{L} \\
 &+ [0.739 (\rho_h f_{yh})^2 + 0.739 (\rho_{vi} f_{yvi})^2] \frac{d}{L} \\
 &+ (0.0875 \sigma_o) \frac{d}{L} \\
 &(r_c = 1 + \langle ar - 1 \rangle - \langle ar - 3 \rangle)
 \end{aligned}$$

Equation U:

$$\begin{aligned}
 v_u &= 0.083 C_d \sqrt{f'_m} \\
 &+ \rho_h f_{yh} \\
 &(C_d = 2.4 + 1.6 \langle ar_d - 1 \rangle - 1.6 \langle ar_d - 0.25 \rangle)
 \end{aligned}$$

Note that equation U does not consider the effect of axial load on shear strength (there is no third term in this case).

3.3 Notation

The definitions of the terms used in this paper are given below. Actual rather than nominal dimensions are used in these definitions.

- A = (L)(t): gross horizontal area of wall (mm²)
- A_h = area of horizontal reinforcement in one layer (mm²)
- A_{vi} = area of vertical reinforcement in one interior core (mm²)
- A_{ve} = area of vertical reinforcement in one end core (mm²)
- d = L - d' = distance of centroid of vertical reinforcement in an end core to the opposite face of wall (mm)
- d' = cover of the centroid of vertical reinforcement in an end core (mm)
- f'_m = compressive strength of masonry from prism tests (MPa)
- f_{yh} = yield strength of horizontal reinforcement (MPa)
- f_{yv} = average yield strength of vertical reinforcement (MPa)

f_{yvi}	=	yield strength of vertical reinforcement in interior cores (MPa)
h	=	height of wall (mm)
L	=	length of wall (mm)
M	=	maximum bending moment that occurs simultaneously with shear force V (N-m)
Q	=	axial load on masonry wall (N)
r	=	h/L = aspect ratio of wall
r_c	=	a discontinuous function of αr (see Appendix B)
r_d	=	$h/d = rL/d$
s_h	=	spacing between layers of uniformly distributed horizontal reinforcement (mm)
s_{vi}	=	spacing of vertical reinforcement in the interior cores (mm)
t	=	thickness of wall (mm)
V	=	shear force on horizontal section of wall (N)
V_u	=	ultimate shear force on horizontal section (N)
v_m	=	contribution of vertical reinforcement to ultimate shear strength (MPa)
v_q	=	contribution of axial load to ultimate shear strength (MPa)
v_s	=	contribution of the horizontal steel to ultimate shear strength (MPa)
v_u	=	V_u/tL : nominal ultimate shear stress (MPa)
α	=	$M/VLr = M/Vdr_d$
δ	=	1.0 for inflection point at mid-height, 0.6 for cantilever type bending

ratio

$$\rho_h = A_h / s_h t \quad (= \Sigma A_h / ht \text{ for subset B}) = \text{horizontal reinforcement ratio}$$

$$\rho_v = (2 A_{ve} + \Sigma A_{vi}) / tL = \text{total vertical reinforcement ratio}$$

$$\rho_{ve} = A_{ve} / tL = \text{ratio of vertical reinforcement in one end core}$$

$$\rho_{vi} = A_{vi} / s_{vi} t = \text{ratio of uniformly distributed vertical reinforcement in the interior cores}$$

$$\sigma_o = Q / A = \text{nominal axial stress on wall (MPa)}$$

4. METHODOLOGY

Each equation was used to predict the ultimate shear strength of all 62 test specimens, using appropriate specimen characteristics such as wall dimensions, masonry strength, steel area, and axial load. The predicted strength was then compared to the actual tested strength. The comparisons were grouped by equation and by pairings of equation and data subset. For example, predicted values versus test results for equation S were grouped into five sets: equation S versus test results from all specimens (S + M + O + B), subset S, subset M, and so on. These grouping of comparisons are referred to in this report using the format X-Y, where X is the equation identification and Y is the data set. For example, S-M refers to the comparison of the predictions by equation S with test results of subset M, while M-S refers to the comparison of predictions by equation M with results of subset S.

Figures 1 through 5 show plots of test-versus-predicted strength. The straight line represents perfect correlation. Points deviating from this line indicate both the scatter in test results and approximations in the predictive formulation. The spread of points above and below this line illustrates tendencies to over- or under-predict as well as general scatter in the test results.

Normalized plots were created by plotting on the y axis the ratio of test to predicted strength for each of the 62 specimens, which are identified by numbers along the x axis. These plots (Figures 6 through 9) are useful in identifying specific pairs or groups of specimens for further investigation.

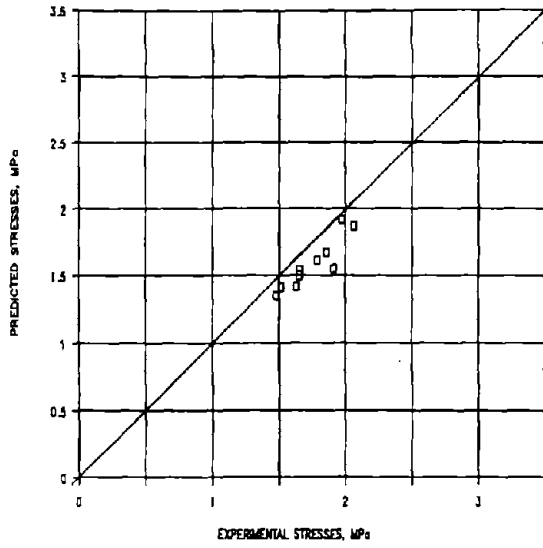
A sample mean, \bar{x}_m , deviation, s , and variation, v , were calculated for each group of comparisons, using the formulae:

$$s = \sqrt{\frac{\sum_1^n (x_i - y_i)^2}{(n - 1)}}, \quad x_m = \frac{\sum x_i}{n}, \quad v = \frac{s}{x_m} \quad (5)$$

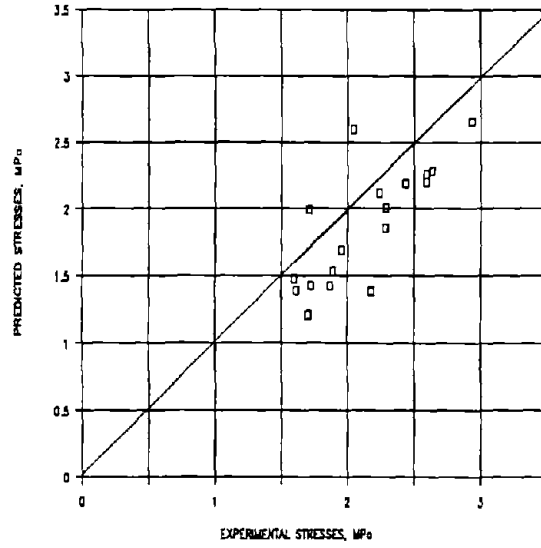
where

x_i	=	ith test value
y_i	=	ith predicted value
n	=	sample size

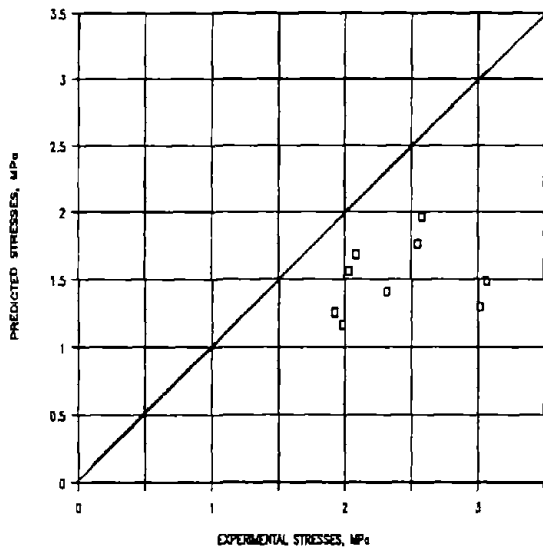
S-S COMPARISON



S-M COMPARISON



S-O COMPARISON



S-B COMPARISON

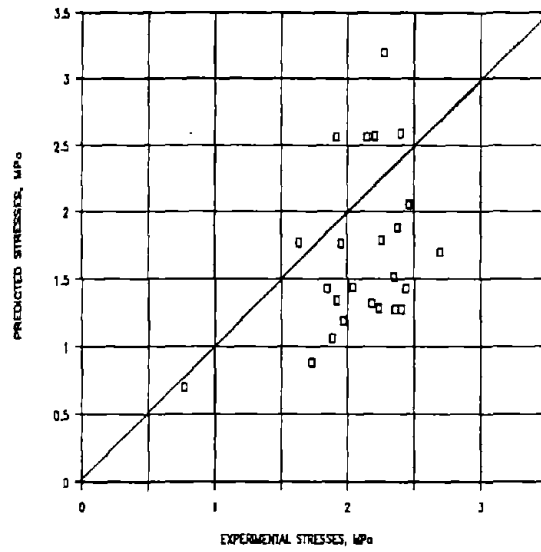


FIGURE 1: EXPERIMENTAL VS PREDICTED STRENGTH: EQUATION S

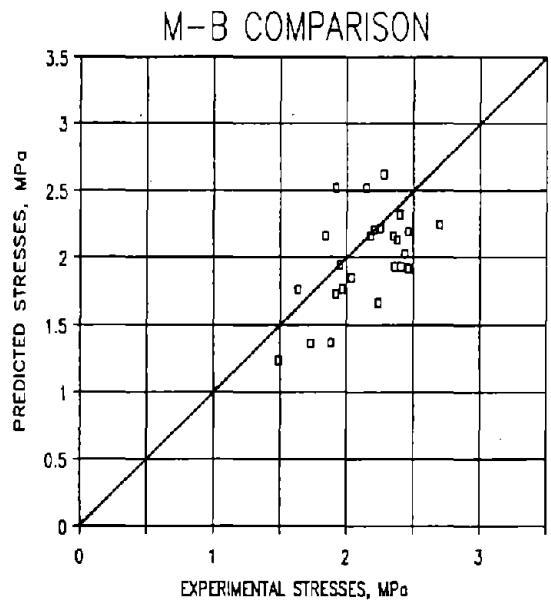
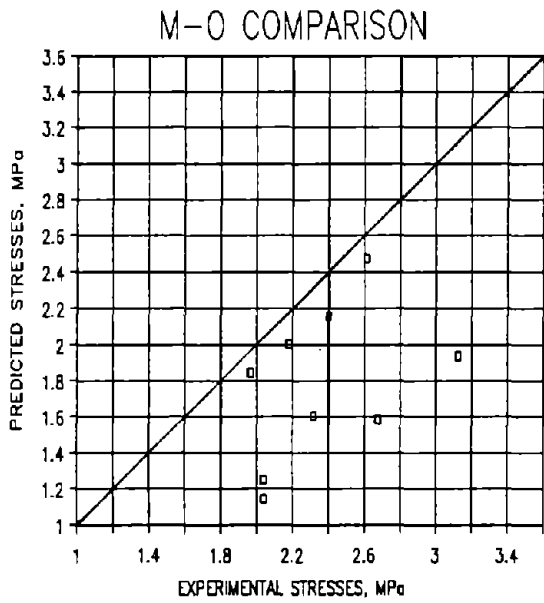
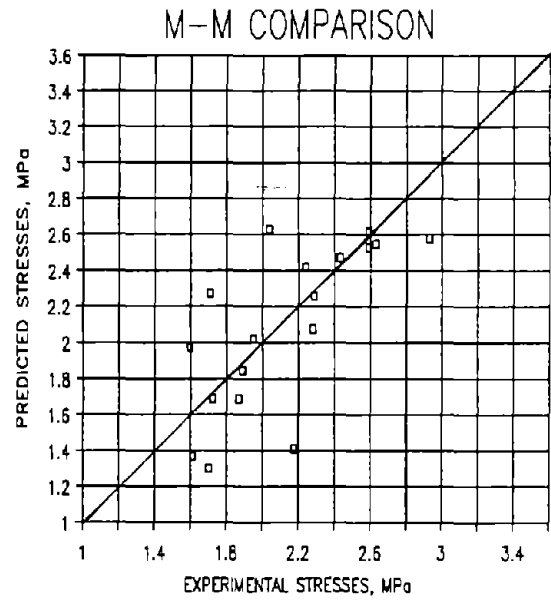
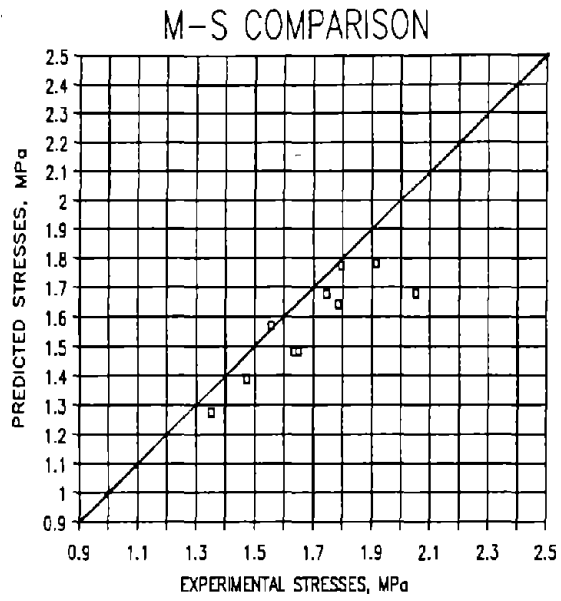


FIGURE 2: EXPERIMENTAL VS PREDICTED STRENGTH: EQUATION M

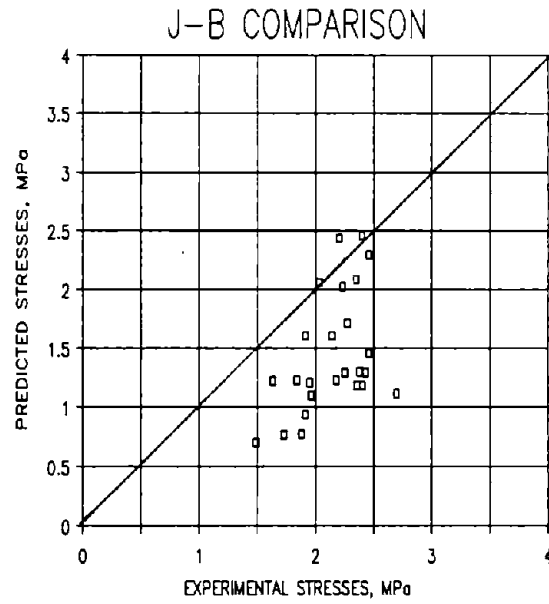
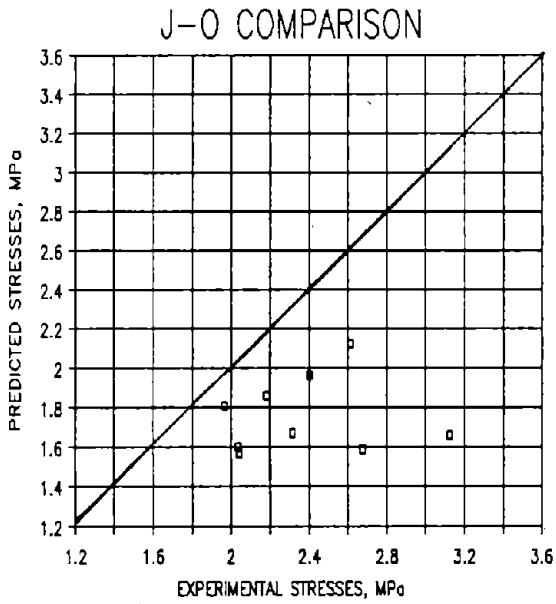
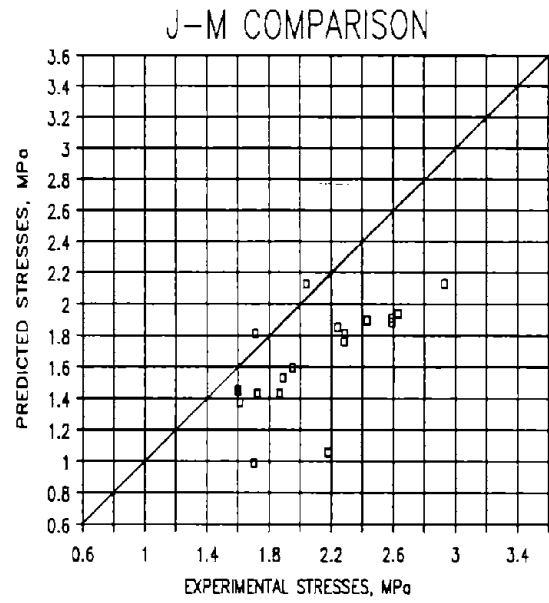
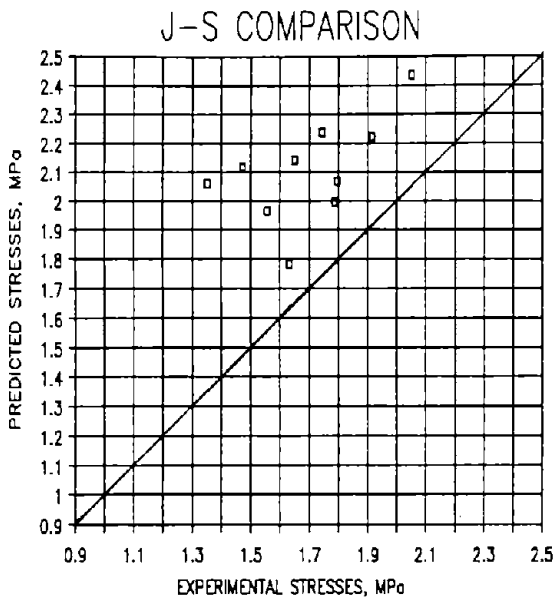


FIGURE 3: EXPERIMENTAL VS PREDICTED STRENGTH: EQUATION J

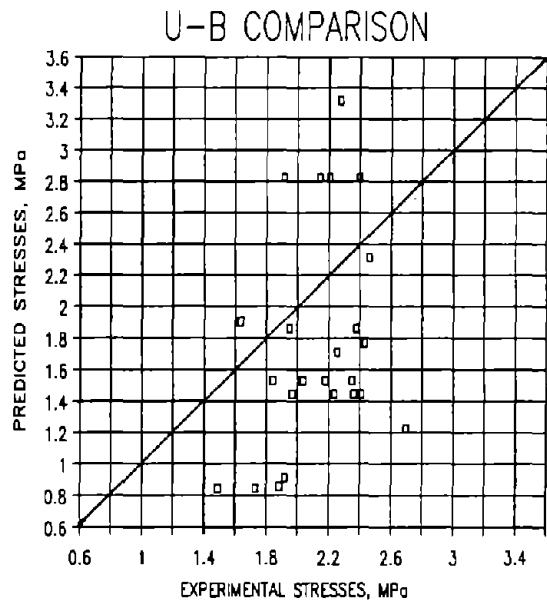
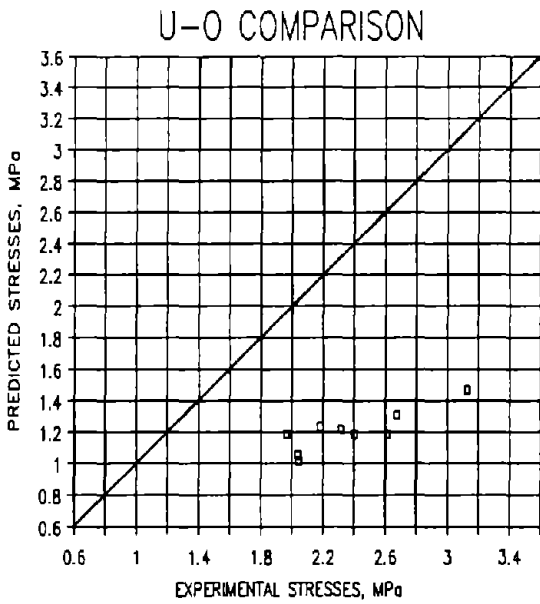
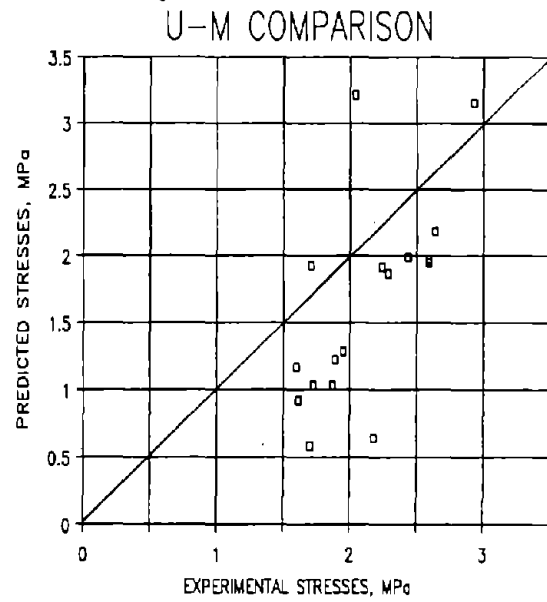
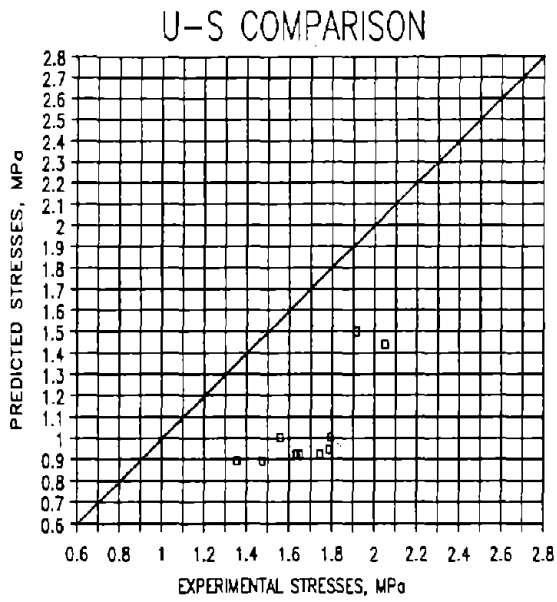


FIGURE 4: EXPERIMENTAL VS PREDICTED STRENGTH: EQUATION U

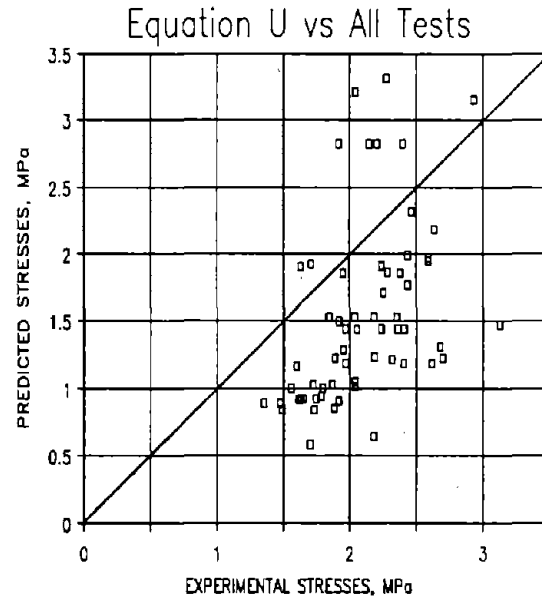
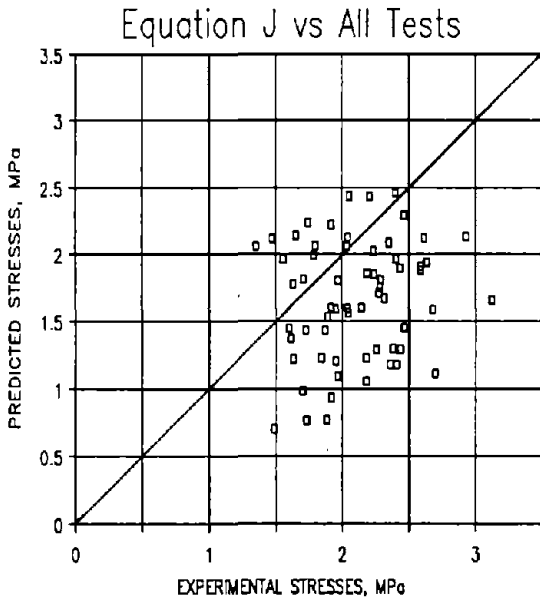
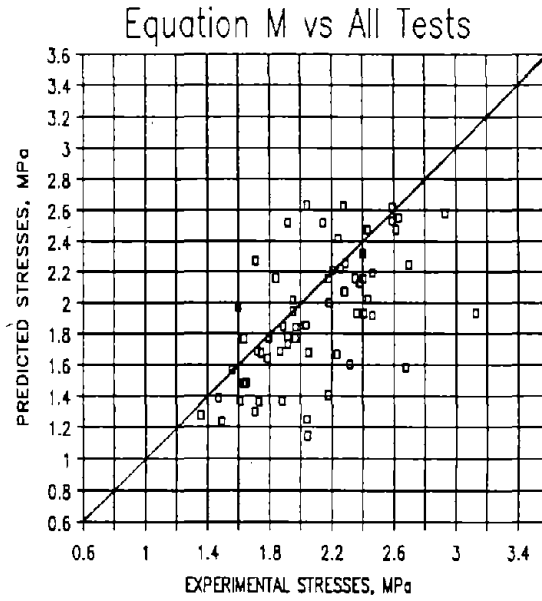
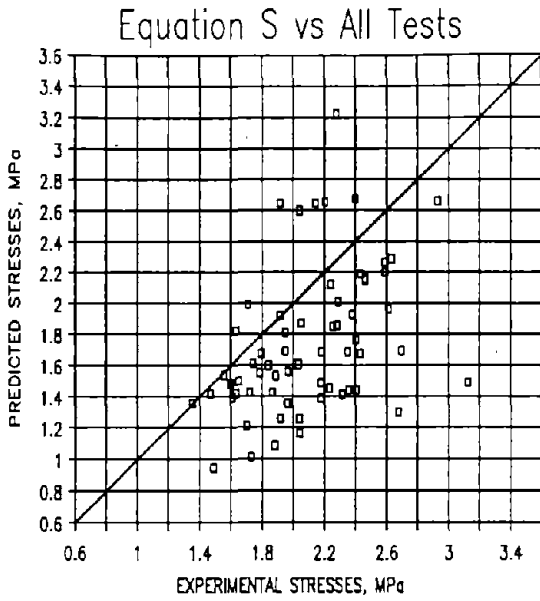


FIGURE 5: EXPERIMENTAL VS PREDICTED STRENGTH: ALL 62 DATA POINTS

The equation for calculating deviation is similar to that used for standard deviation, but the numerical value of deviation cannot be used in statistical analysis because the data points being evaluated do not represent repetitive tests and the scatter is due to multiple causes. Likewise, variation is defined in the same way as coefficient of variation in statistics, but for the same reasons, does not have the same meaning. However, those indicators as defined and calculated here are useful for making comparisons of the predictive accuracy of the four equations.

To carry the comparisons of the equations one step further, the relative contribution of each of the three strength terms (v_m , v_s , and v_q) was examined. The values of each of the three terms contributing to the prediction of each equation for all 62 specimens were tabulated (Table 2). Histograms were produced that presented information from all four equations on one plot for each of the three terms, and for the combined ultimate shear strength (Figures 10 through 13).

The effects of specific parameters were investigated by identifying specimens that essentially differed in only one parameter. The ratios of test to predicted values for these similar specimens were compared (Figures 6 through 9). Similar ratios indicate that the predictive equation effectively accounts for the varying parameter. Divergent ratios indicate the opposite.

5. RESULTS AND ANALYSIS

5.1 Results

Table 2 lists the actual strengths determined from tests of all 62 specimens, and the predicted strengths (v_m , v_s , v_q and the sum v_u) obtained from each formula. Graphical comparisons of predicted and test results are shown in Figures 1 through 4, each of which contains four data plots. Figure 5 shows the test/prediction plot for each of the four equations for all 62 data points.

Figures 1 through 5 vividly illustrate the fact that none of the equations is able to precisely predict the ultimate shear strength of all the specimens. However, part of the scatter is due to the variability of strength inherent in masonry construction. A study by Blume and Proulx [8] suggests the magnitude of inherent variation that can be expected. Test results from 84 diagonally-loaded shear walls, in replicate groups of 4 and 5, gave a range of coefficient of variation (standard deviation divided by sample mean) of 3-18%. The large spread in the coefficient of variation is attributed primarily to the small sample size. The average coefficient of variation for all the replicate tests was 8%. The Blume and Proulx study suggests that variation of about 10% between

TABLE 2. PREDICTIONS OF V_m , V_s , V_q , AND V_u AND TEST V_u

TEST NUMBER	V_m				V_s				V_q				$V_u =$ MPa	$V_m + V_q + V_s$			V_u TESTS MPa
	S	M	J	U	S	M	J	U	S	M	J	U		S	M	J	
1	1.12	1.09	0.33	0.45	0.31	0.28	1.75	0.47	0.18	0.31	0.15	0.00	1.61	1.68	2.24	0.92	1.74
2	1.04	1.02	0.31	0.42	0.31	0.26	1.75	0.47	0.00	0.00	0.00	0.00	1.35	1.28	2.08	0.89	1.35
3	1.04	1.02	0.31	0.42	0.31	0.26	1.75	0.47	0.06	0.11	0.08	0.00	1.42	1.39	2.12	0.89	1.47
4	1.12	1.09	0.33	0.45	0.31	0.28	1.75	0.47	0.07	0.11	0.08	0.00	1.50	1.48	2.14	0.92	1.65
5	0.92	0.90	0.29	0.45	0.31	0.28	1.34	0.47	0.18	0.31	0.15	0.00	1.42	1.48	1.78	0.92	1.63
6	1.04	1.04	0.33	0.47	0.31	0.29	1.74	1.03	0.19	0.31	0.15	0.00	1.92	1.78	2.22	1.50	1.91
7	1.04	1.04	0.33	0.47	0.31	0.29	1.51	0.47	0.19	0.31	0.15	0.00	1.55	1.64	1.99	0.95	1.79
8	1.02	1.00	0.30	0.41	0.31	0.28	1.98	1.03	0.17	0.31	0.15	0.00	1.87	1.68	2.44	1.44	2.05
9	1.13	1.13	0.36	0.51	0.33	0.32	1.55	0.49	0.21	0.32	0.16	0.00	1.68	1.77	2.07	1.00	1.79
10	1.13	1.13	0.36	0.51	0.33	0.32	1.55	0.49	0.08	0.11	0.06	0.00	1.54	1.57	1.96	1.00	1.56
11	1.14	1.43	0.44	0.71	0.29	0.47	0.97	0.45	0.05	0.08	0.04	0.00	1.48	1.97	1.45	1.17	1.60
12	1.14	1.15	0.43	0.58	0.23	0.46	0.96	0.45	0.05	0.08	0.04	0.00	1.43	1.69	1.43	1.03	1.72
13	1.14	1.15	0.43	0.58	0.23	0.46	0.96	0.45	0.05	0.08	0.04	0.00	1.43	1.69	1.43	1.03	1.87
14	1.22	0.85	0.39	0.47	0.12	0.44	0.95	0.45	0.05	0.08	0.04	0.00	1.39	1.37	1.37	0.92	1.61
15	1.01	0.98	0.39	0.58	0.00	0.00	0.44	0.00	0.20	0.32	0.16	0.00	1.21	1.30	0.99	0.58	1.70
16	1.01	0.98	0.39	0.58	0.32	0.55	0.99	0.64	0.20	0.32	0.16	0.00	1.53	1.85	1.53	1.23	1.89
17	1.01	0.98	0.39	0.58	0.65	0.78	1.22	1.29	0.20	0.32	0.16	0.00	1.86	2.07	1.76	1.87	2.28
18	1.16	1.17	0.44	0.58	0.65	0.78	1.22	1.29	0.20	0.32	0.16	0.00	2.01	2.26	1.81	1.87	2.29
19	1.16	1.17	0.44	0.58	1.30	1.10	1.54	2.57	0.20	0.32	0.16	0.00	2.66	2.58	2.13	3.15	2.93
20	1.33	1.33	0.51	0.66	0.65	0.89	1.22	1.29	0.23	0.32	0.16	0.00	2.20	2.53	1.89	1.95	2.59
21	1.26	1.26	0.48	0.63	0.65	0.84	1.22	1.29	0.22	0.32	0.16	0.00	2.12	2.42	1.85	1.92	2.24
22	1.29	1.29	0.49	0.65	0.78	0.94	1.29	1.54	0.22	0.32	0.16	0.00	2.29	2.55	1.94	2.19	2.63
23	1.29	1.29	0.49	0.63	0.69	0.87	1.25	1.36	0.22	0.32	0.16	0.00	2.19	2.47	1.90	1.99	2.43
24	1.38	1.38	0.54	0.69	0.65	0.92	1.22	1.29	0.24	0.32	0.16	0.00	2.27	2.62	1.91	1.98	2.59
25	1.16	1.10	0.45	0.64	0.00	0.00	0.48	0.00	0.23	0.31	0.16	0.00	1.39	1.41	1.08	0.64	2.18
26	1.16	1.10	0.45	0.64	0.30	0.81	0.99	0.64	0.23	0.31	0.16	0.00	1.69	2.02	1.59	1.29	1.95
27	1.16	1.10	0.45	0.64	0.61	0.86	1.21	1.29	0.23	0.31	0.16	0.00	1.99	2.27	1.82	1.93	1.71
28	1.16	1.10	0.45	0.64	1.21	1.22	1.53	2.57	0.23	0.31	0.16	0.00	2.60	2.63	2.13	3.21	2.04
29	0.88	1.10	0.31	0.72	0.42	0.49	1.28	0.59	0.00	0.00	0.00	0.00	1.30	1.59	1.59	1.31	2.68
30	1.06	1.00	0.39	0.59	0.30	0.53	1.26	0.59	0.20	0.32	0.16	0.00	1.56	1.84	1.81	1.19	1.97
31	1.01	0.69	0.32	0.42	0.16	0.45	1.25	0.59	0.00	0.00	0.00	0.00	1.16	1.14	1.57	1.01	2.04
32	1.06	1.00	0.39	0.59	0.30	0.53	1.26	0.59	0.41	0.63	0.32	0.00	1.76	2.16	1.97	1.19	2.40
33	1.06	1.00	0.39	0.59	0.30	0.53	1.26	0.59	0.61	0.95	0.47	0.00	1.97	2.48	2.12	1.19	2.61
34	1.07	1.34	0.39	0.88	0.42	0.60	1.27	0.59	0.00	0.00	0.00	0.00	1.49	1.94	1.66	1.47	3.12
35	1.11	1.05	0.41	0.62	0.30	0.56	1.26	0.59	0.00	0.00	0.00	0.00	1.41	1.61	1.67	1.22	2.32
36	1.10	0.76	0.35	0.48	0.16	0.49	1.25	0.59	0.00	0.00	0.00	0.00	1.28	1.25	1.60	1.05	2.04
37	1.14	1.08	0.43	0.64	0.30	0.58	1.26	0.59	0.24	0.35	0.17	0.00	1.69	2.00	1.86	1.24	2.18
38	0.88	0.88	0.31	0.72	0.73	0.76	0.74	1.14	0.20	0.31	0.15	0.00	1.81	1.95	1.21	1.86	1.95
39	0.88	0.88	0.31	0.72	0.73	0.76	0.74	1.14	0.31	0.49	0.25	0.00	1.93	2.13	1.30	1.86	2.38
40	0.81	0.97	0.32	0.60	1.10	0.77	0.91	1.72	0.24	0.45	0.23	0.00	2.15	2.19	1.45	2.32	2.48
41	0.82	0.70	0.25	0.60	1.10	0.77	1.82	1.72	0.24	0.45	0.23	0.00	2.16	1.92	2.30	2.32	2.48
42	0.79	0.95	0.31	0.58	0.42	0.53	0.64	0.86	0.23	0.45	0.23	0.00	1.44	1.93	1.18	1.44	2.38
43	0.80	0.68	0.24	0.58	0.42	0.53	1.56	0.86	0.23	0.45	0.23	0.00	1.45	1.67	2.02	1.44	2.23
44	0.79	0.95	0.31	0.58	0.23	0.33	0.40	0.33	0.23	0.45	0.23	0.00	1.28	1.73	0.94	0.91	1.92
45	0.79	0.95	0.31	0.58	0.65	0.63	0.76	1.19	0.23	0.45	0.23	0.00	1.68	2.03	1.29	1.77	2.43
46	0.79	0.95	0.31	0.58	0.42	0.53	0.64	0.86	0.15	0.28	0.14	0.00	1.36	1.77	1.10	1.44	1.96
47	0.79	0.95	0.31	0.58	0.42	0.53	0.64	0.86	0.23	0.45	0.23	0.00	1.44	1.93	1.18	1.44	2.40
48	0.91	1.09	0.36	0.67	0.42	0.61	0.64	0.86	0.27	0.45	0.23	0.00	1.60	2.16	1.23	1.53	1.84
49	0.91	1.09	0.36	0.67	1.46	0.97	1.02	2.15	0.27	0.45	0.23	0.00	2.65	2.52	1.60	2.82	1.92
50	1.00	1.09	0.36	0.67	0.42	0.61	1.50	0.86	0.27	0.45	0.23	0.00	1.69	2.16	2.09	1.53	2.35
51	0.94	0.90	0.31	0.67	1.46	0.97	1.93	2.15	0.27	0.45	0.23	0.00	2.67	2.32	2.46	2.82	2.40
52	0.92	0.78	0.28	0.67	0.42	0.61	1.56	0.86	0.27	0.45	0.23	0.00	1.61	1.85	2.06	1.53	2.03
53	0.92	0.79	0.28	0.67	1.46	0.97	1.93	2.15	0.27	0.45	0.23	0.00	2.65	2.21	2.44	2.82	2.20
54	0.80	1.09	0.36	0.67	0.42	0.61	0.64	0.86	0.27	0.45	0.23	0.00	1.49	2.16	1.23	1.53	2.18
55	0.91	1.09	0.36	0.67	1.46	0.97	1.02	2.15	0.27	0.45	0.23	0.00	2.65	2.52	1.60	2.82	2.14
56	0.91	1.09	0.36	0.67	0.67	0.68	0.71	1.04	0.27	0.45	0.23	0.00	1.85	2.22	1.29	1.71	2.25
57	0.92	1.09	0.36	0.67	2.04	1.08	1.13	2.65	0.27	0.45	0.23	0.00	3.22	2.62	1.71	3.32	2.27
58	1.07	1.28	0.43	0.79	0.31	0.51	0.46	0.44	0.31	0.45	0.23	0.00	1.69	2.25	1.12	1.22	2.69
59	0.74	0.70	0.25	0.62	0.07	0.29	0.33	0.22	0.14	0.25	0.12	0.00	0.94	1.24	0.70	0.84	1.49
60	0.74	0.70	0.25	0.62	0.88	0.69	0.79	1.29	0.21	0.38	0.19	0.00	1.82	1.77	1.22	1.91	1.63
61	0.74	0.70	0.25	0.62	0.07	0.29	0.33	0.22	0.21	0.38	0.19	0.00	1.01	1.36	0.77	0.84	1.73
62	0.74	0.70	0.25	0.62	0.14	0.30	0.34	0.23	0.21	0.38	0.19	0.00	1.08	1.37	0.77	0.85	1.88

test and predicted strength could be attributed to the inherent variability of masonry construction.

Table 3 presents the deviations which were calculated for each of the comparisons. The deviations from the data subsets must be considered closely in evaluating the deviation from the total data set because sample sizes and test scatter of the subsets are different. The correlations with subsets, especially cross-correlations, are meaningful in assessing inconsistencies in the predictive equations.

Table 3 - Deviation (s), Mean (x), and Variation (v) in predicted vs test strengths (MPa)

DATA SET	STATS	EQUATION			
		S	M	J	U
S	s	0.146	0.165	0.466	0.701
	x	1.695	1.695	1.695	1.695
	v	0.086	0.097	0.275	0.414
M	s	0.389	0.332	0.563	0.745
	x	2.125	2.125	2.125	2.125
	v	0.183	0.156	0.265	0.351
O	s	1.000	0.762	0.767	1.267
	x	2.373	2.373	2.373	2.373
	v	0.421	0.321	0.323	0.534
B	s	0.643	0.345	0.845	0.752
	x	2.143	2.143	2.143	2.143
	v	0.300	0.161	0.394	0.351
TOTAL	s	0.582	0.397	0.692	0.813
	x	2.099	2.099	2.099	2.099
	v	0.277	0.189	0.330	0.387

The magnitude of the deviations in Table 3 can be considered in light of the Blume and Proulx study. An examination of the range of tested strengths (presented in Table 1) and deviations is instructive. The actual tested strengths varied from 1.35-3.12 MPa (196-453 psi) with 85% falling between 1.52-2.59 MPa (220-376 psi). The average strength of the 62 specimens is 2.10 MPa (305 psi). A deviation of 0.69 MPa (100 psi) is about 1/3 of the average strength (eight deviations in Table 3, exclusive of comparisons with all the tests, were greater than 0.69 MPa (100 psi)). A deviation of this magnitude cannot be attributed to natural variation in strength of masonry construction. However, a deviation of 0.15 or 0.17 MPa (the best in this study) is about 7% of the average value, and is certainly an acceptable deviation in light of the Blume and Proulx study.

The deviations in Table 3 show that some equations are more successful in predicting ultimate shear strength than others. The table also shows that some data sets are more accurately predicted than others. An evaluation of the data sets to identify the factors that contribute to the success of the predictions follows.

5.2 Analysis of Data

Table 3 (deviation) shows that none of the four equations was very successful in predicting the strengths of data set O. The plots for the comparisons against data set O shown in Figures 1 through 4 indicate that all four equations underestimated the actual test strengths. This consistent underprediction suggests that the specimens of data set O, for whatever reason, developed higher than normal strengths. To determine if this was indeed the case, additional comparisons were made. Specimens WS1 and WSR1 from data set O (test numbers 29 and 34) share similar characteristics with specimen KW4-1 (test number 11) of data set M except for magnitude of axial stress and ρ_v . The two specimens of group O had zero axial stress and $\rho_v = 0.005$; the specimen of group M had an axial stress of 0.49 MPa (71 psi) and $\rho_v = 0.009$. The ultimate shear strengths reported from the actual test results were 2.67 and 3.12 MPa (388 and 453 psi) for the O specimens, but only 1.60 MPa (232 psi) for the M specimen. The fact that these two group O specimens, in spite of the absence of axial load and the lighter vertical reinforcement, developed about twice as much strength as the group M specimen confirms the possibility that the specimens of group O generally may have developed substantially higher strengths than the specimens of group M of similar construction. Similar comparisons with the results of data set S indicate the same trend (e.g. compare results of 22-S and WS1-O). The overstrength of these specimens makes the results from data set O less typical than the other data sets in evaluating predictive capabilities of the four equations.

It should be noted that data set B includes specimens with variations in type of anchorage of horizontal reinforcement and the distribution of horizontal and vertical bars in addition to the variation of parameters tabulated in Appendix A. These variations contribute to the scatter evident in the plots of test-versus-predicted strengths.

The normalized plots of Figures 6 through 9, representing equations S, M, J, and U, respectively, show the ratios of test strength to predicted strength (v_{ur}/v_{up}) according to the test number. The four data subsets are identified by their symbols appearing at the top in these figures. Data subsets S, M, O and B correspond to test numbers 1-10, 11-28, 29-37 and 38-62, respectively. Prediction underestimates and overestimates can be readily identified according to whether the line plotting the ratio of test to predicted value falls above or below the unity line, respectively. These plots clearly show the tendency of all the equations to underestimate the unusually high test strength of data set O, and also confirm the erratic nature of predictions of the results of data set B.

Table 3 shows that three of the four equations (S, M, and J) were more successful in predicting the strengths of data set S than of any other. Plausible reasons for the generally small deviations are (1) the horizontal and vertical reinforcement in the specimens of group S were distributed more uniformly than was typical in the specimens of the other data sets, and (2) several parameters (r , d , d' , and s_h) in the S test series were not varied, and the range of most of those that were varied (ρ_h , ρ_v , σ_o) was narrow relative to the other test series. Equation U consistently underestimated data set S by considerable margins. Equation U gives substantially less weight to the strength component v_m than equations S and M (Figure 10). It also ignores the contribution of axial load on strength ($v_q = 0$).

Equation S

This formula was developed to fit the test data of group S using regression analysis. Consequently, predictions by equation S were in closer agreement with results of data set S than any other comparison.

Shing et al [2,3], note that experimental observations indicate that the post-cracking strength of masonry increases with vertical steel and axial load, mainly through resistance at the compression face, aggregate interlock and dowel action. These contributions to v_q are represented by the first and third terms of equation S. The contribution of horizontal steel, reflected by the second term of equation S, takes into account the ineffectiveness of the top and bottom layers of horizontal steel due to insufficient embedment length to develop their yield capacity following diagonal shear rupture.

FIGURE 6. EQUATION S STRENGTH RATIOS
EXPERIMENTAL/PREDICTED

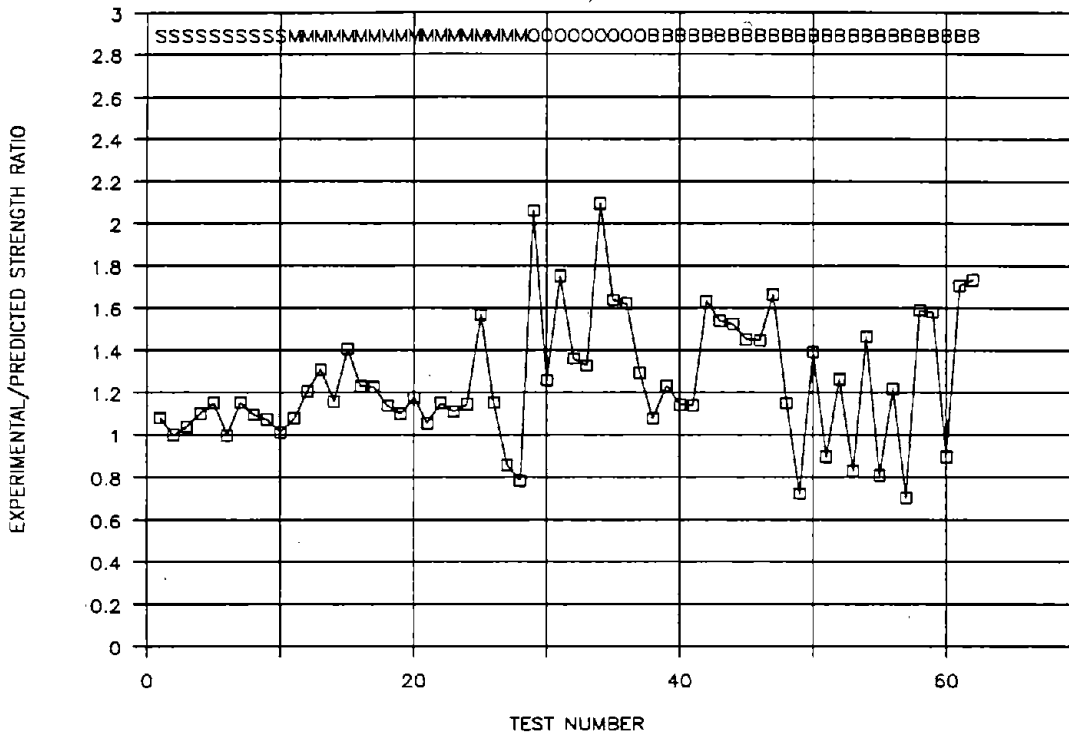


FIGURE 7. EQUATION M STRENGTH RATIOS
EXPERIMENTAL/PREDICTED

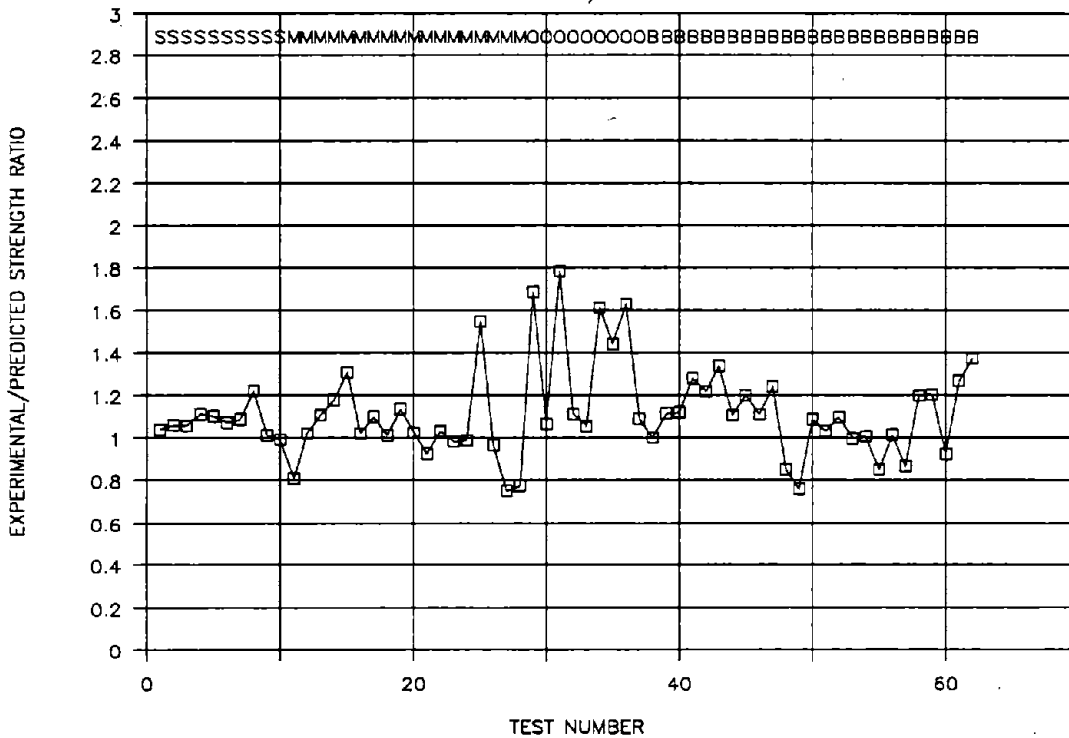


FIGURE 8. EQUATION J STRENGTH RATIOS

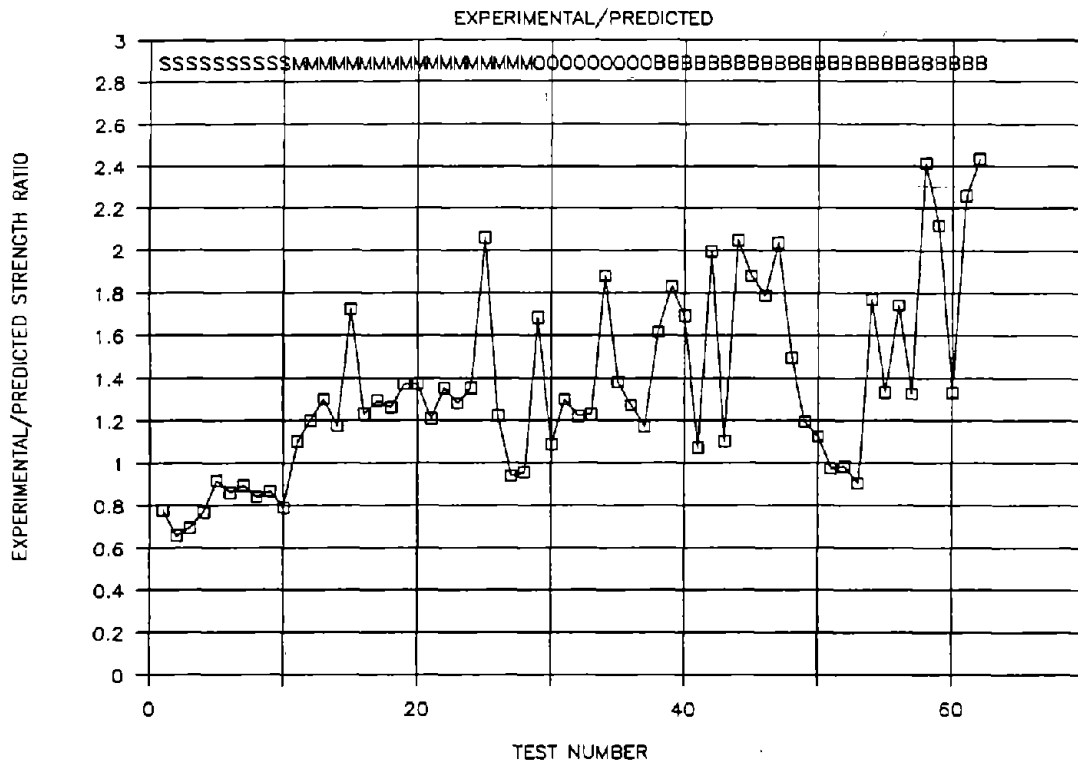
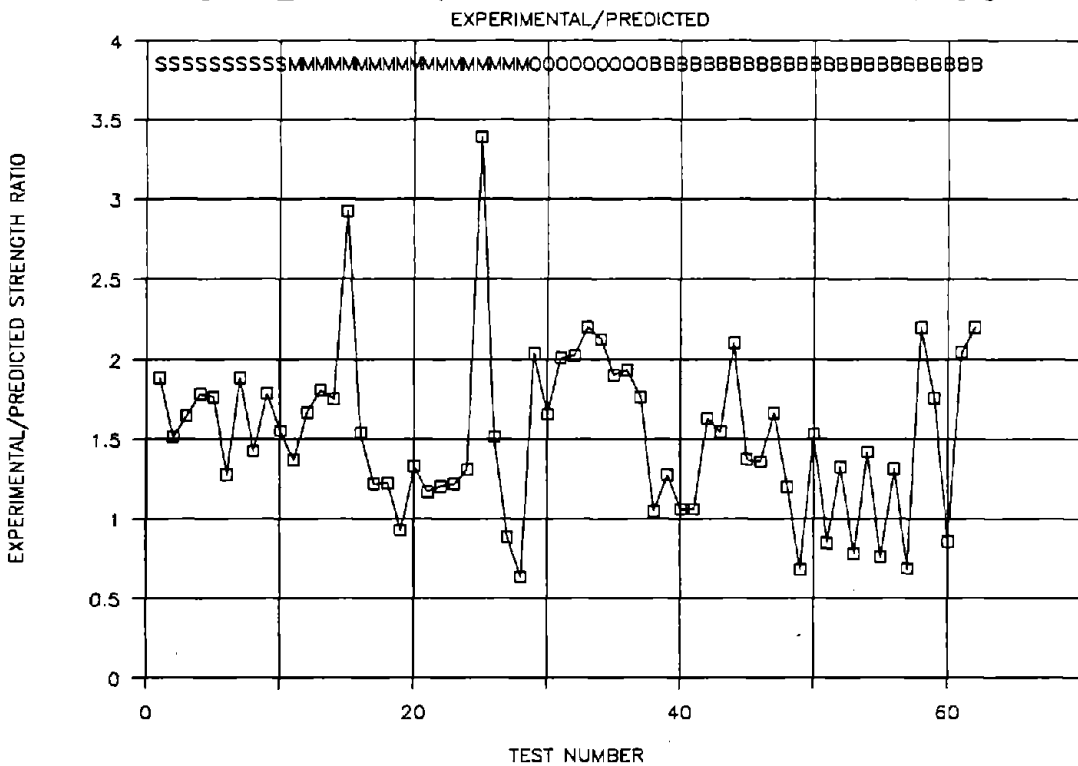


FIGURE 9. EQUATION U STRENGTH RATIOS



Shing et al demonstrated that their proposed formula is in better agreement with their test results than the UBC formula, which they showed to be consistently more conservative. This conclusion is verified in this study, which showed the deviation of predictions by equation U of data set S to be five times the deviation of predictions by equation S of the same data set (0.70 versus 0.15 MPa or 102 versus 21 psi respectively), with equation U consistently underpredicting the strength of the specimens of group S.

Equation M

In reference [4], Matsumura describes the development of the formula presented in this paper as equation M (original form is shown in Appendix B). Matsumura developed this formula by utilizing his test results (data set M in this study) as well as test results reported by other researchers in Japan. He, like Shing et al, used regression analysis to determine the appropriate functional forms of the parameters.

Overall, equation M is the most successful of the four equations. Equations M and S are comparable in accuracy in predicting data sets S and M, but equation M is the most successful of the four equations in predicting the test results of group B specimens.

Equation J

Equation J is based on a formula published in the Reinforced Concrete Design Standard of the Architectural Institute of Japan for predicting the ultimate shear strength of concrete shear walls. The predicted strength for specimen WSRC-O, the concrete wall, was about 85% of test strength. Predictions of masonry shear wall strength by equation J were less successful.

There are notable similarities between equations M and J in the types of parameters considered to have an effect on shear response. A major difference is that equation J considers the contribution of interior vertical bars, which equation M neglects. Another significant difference is that equation M includes the square root of the compressive strength of masonry as a multiplier in the term representing the contribution of horizontal reinforcement; equation J does not.

Equation J was less successful in predicting the strengths of data set S (deviation = 0.46 MPa or 68 psi) than equations S and M. The weight given to the contribution of interior vertical reinforcement (as expressed in steel ratio ρ_{vi}) by equation J partially explains this difference in predictive success. Equation J gives equal weight to ratios of horizontal and interior vertical reinforcement, ρ_h and ρ_{vi} , in the determination of steel contribution to strength.

None of the other equations specifically include the effect of ρ_{vi} in the predicted strength. Equation S includes ρ_v in the v_m term, which incorporates the contribution of all vertical steel. Equation M only includes the steel in the end cores, as measured by ρ_{ve} , in its expression for masonry strength. Equation U does not consider the contribution of vertical steel at all. The v_s terms in Table 2 show that for data set S, predictions of steel contribution to strength by equation J (average 1.67 MPa or 242 psi) far exceed the predictions of the other three equations (average 0.43 MPa or 62 psi). The effect of the ρ_{vi} term in causing the overprediction of data set S is confirmed by examining the magnitudes of ρ_{vi} in all four data sets.

The ranges of ρ_h and ρ_{vi} in data set S are 0.0012 to 0.0022 and 0.0034 to 0.0067, respectively. Because of the relative ratios of horizontal and interior vertical steel in these specimens, the contribution of the interior vertical reinforcement according to equation J will be 2 to 3 times that of the horizontal reinforcement. Figure 8 shows that equation J consistently overpredicted the strength of data set S, while it tended to underpredict the strengths of the other data sets. Only 8 specimens in the other data sets have ρ_{vi} in excess of the minimum value of 0.0034 used in the S series. Equation J predictions of these specimens with lower ρ_{vi} were, on average, even less successful than predictions for data set S (deviations of 0.56, 0.77, and 0.84 MPa or 82, 111, and 122 psi for data sets M, O, and B, respectively). The strengths of 4 of the non-S high- ρ_{vi} specimens are overpredicted by equation J. The overestimation of one data subset and underestimation of the others indicates that the adoption of this equation for masonry shear walls through corrections based on regression constants is not possible.

Equation U

Equation U was the least successful of the four equations in predicting ultimate shear strength. This equation, the formula for ultimate shear strength of masonry shear walls specified in the 1988 Uniform Building Code [7], does not consider the effect of axial load. For three out of the four data subsets (S, M, and O) equation U underestimates the test results, with the exception of three specimens (numbers 19, 27, and 28) having high ρ_h , to which equation U is more sensitive than the other equations.

The closest correlations of equation U, with data sets S and M, correspond to deviations which are 2 to 5 times those corresponding to equations S and M. In most instances, equation U gives strength estimates that are overly conservative, with deviations in excess of 0.69 MPa (100 psi) in every case (see Table 3). In addition, predictions based on equation U generally are not consistent with test results.

5.3 Analysis of Strength Prediction

The deviations in Table 3 clearly show that equation M was the most successful predictor of actual shear strengths. The deviation calculated from the combined data sets, 0.39 MPa (58 psi), is significantly less than the deviations for the other three equations, 0.58, 0.69, and 0.81 MPa (84, 100, and 118 psi) for equations S, J, and U, respectively. Formula S was comparatively successful in predicting the S and M data sets, but it was only slightly better than equation U in predicting data sets O and B. Equation M was the most successful of the four equations in predicting data set B, with a deviation of 0.34 MPa (50 psi), and was by far more successful than equations S and U in predicting the unexpectedly high strength of data set O.

The M-M deviation was almost twice the S-S deviation (0.33 and 0.14 MPa, or 48 psi and 28 psi respectively). This may be attributed to the fact that equation M was calibrated using other data in addition to data subset M, while the equation S was calibrated using only data subset S. Additionally, a wider range of parameters was used in the M series of specimens compared to the S series. The M-S comparison was very successful, with a deviation similar to that for the S-S comparison (0.17 and 0.15 MPa or 24 and 21 psi, respectively). The S-M deviation, 0.39 MPa (56 psi), was comparable to the M-M deviation of 0.33 MPa (48 psi).

To carry the comparisons between formulae one step further, the contribution of the individual terms (v_m , v_s , v_q) were examined. Figures 10 through 13 are histograms comparing the magnitude of the predicted v_m , v_s , v_q , and v_u stresses, respectively, for all 62 tests, following the numerical order of specimens listed in Table 1. Data subsets S, M, O and B are identified by their symbols in the figures.

Figure 10 shows consistently lower estimates of v_m by equation J relative to the predictions by the other equations. Values of v_m from equation U are low relative to predictions by formulas S and M. Values predicted by equations S and M generally exhibit comparable trends for v_m predictions. Figure 11 shows the contribution of v_s terms. The predictions according to equation S and M are generally comparable in

FIGURE 10. PREDICTED V_m STRESSES, MPa

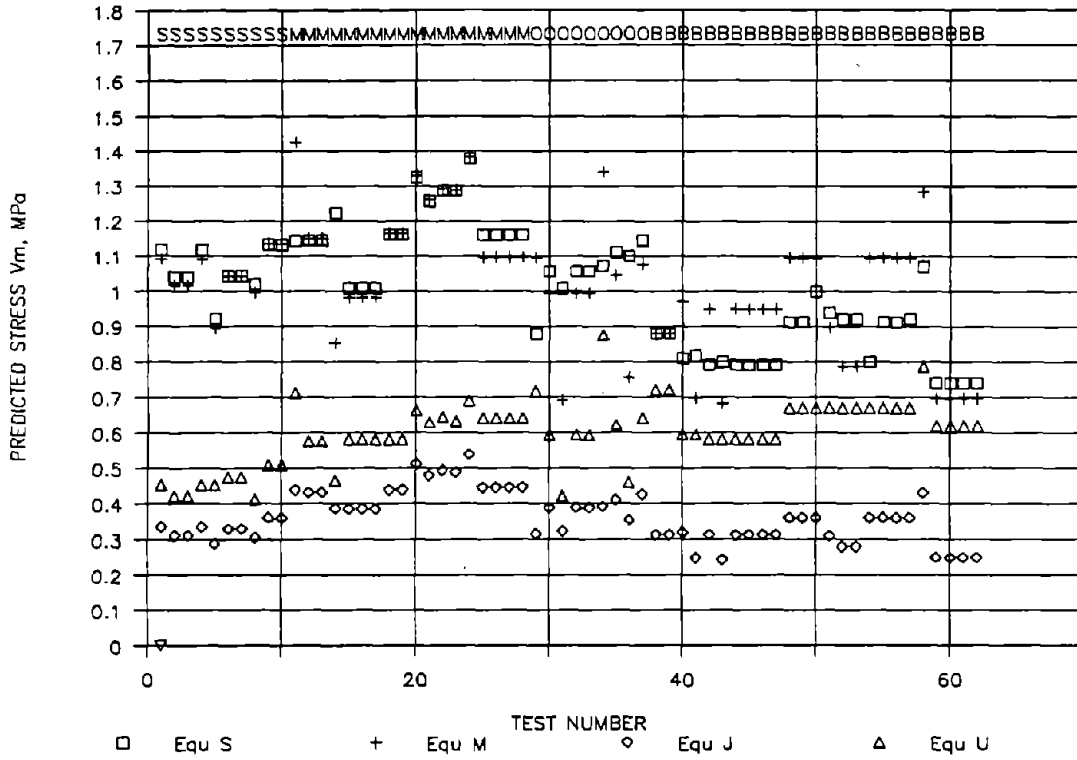


FIGURE 11. PREDICTED V_s STRESSES, MPa

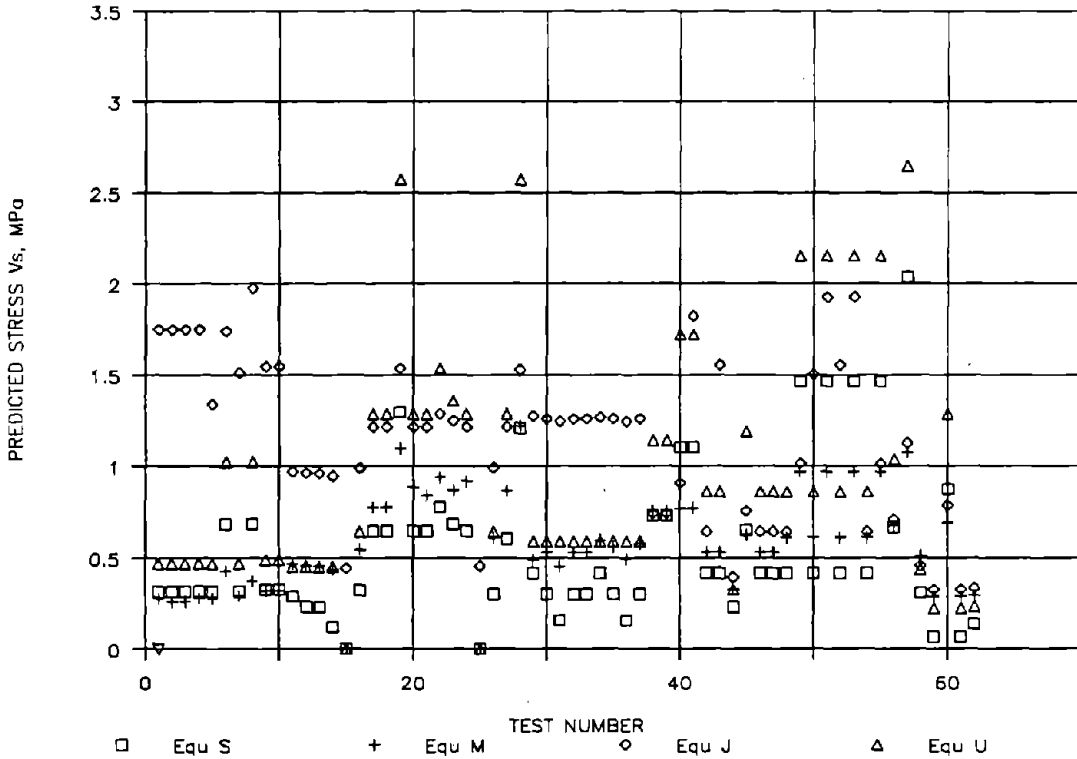


FIGURE 12. PREDICTED V_q STRESSES, MPa

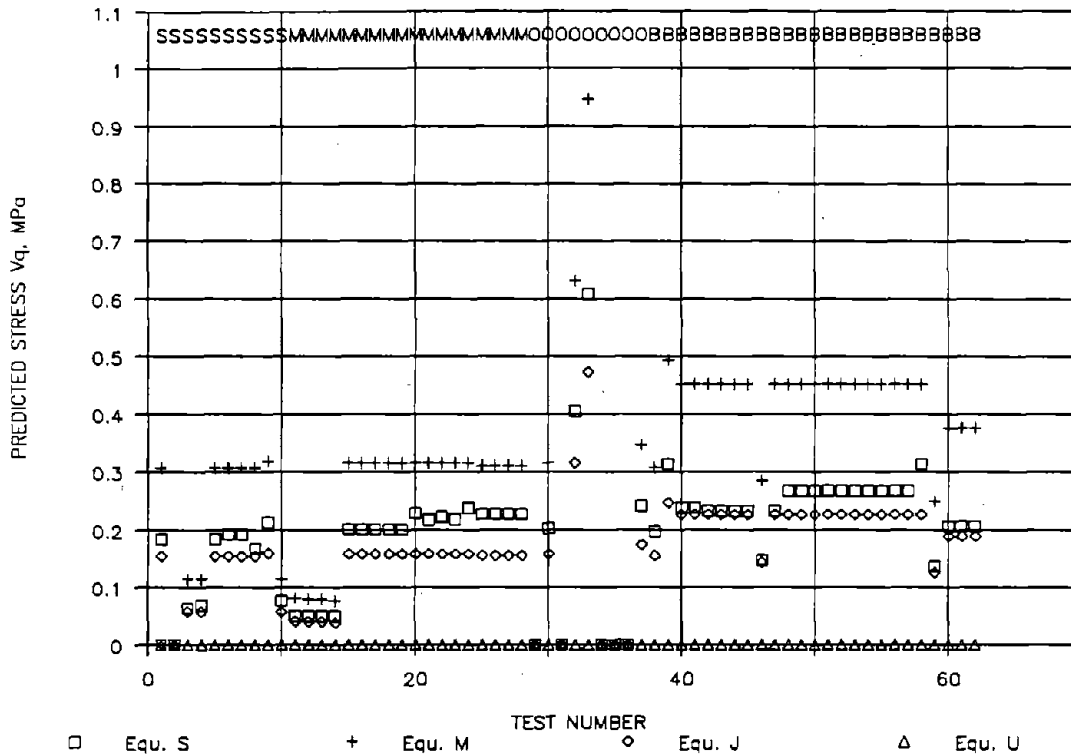
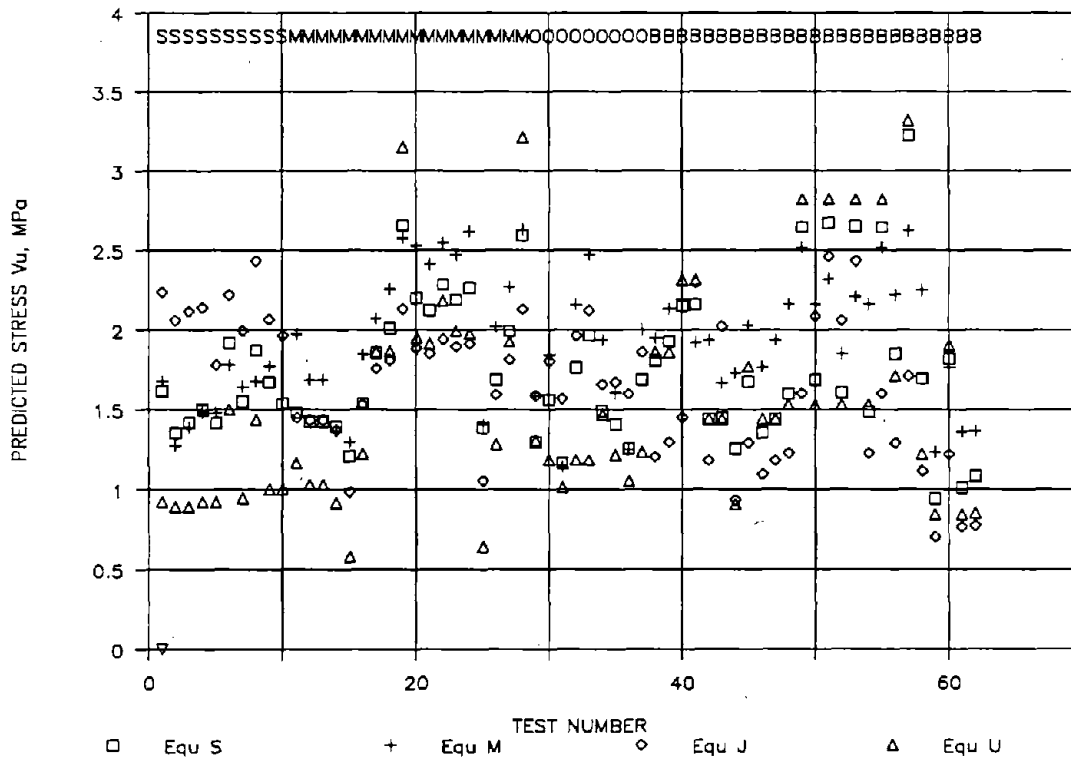


FIGURE 13. PREDICTED V_u STRESSES, MPa



trend and magnitude, while v_s contributions according to equations J and U vary widely. The v_s terms of the four equations are the least similar in form. Figure 12 shows the contribution of the v_q terms. Formula U does not include a term to account for axial load effect, indicated on the plot by a value of zero for all predictions by equation U. The axial load effect in equations J and S is lower than in equation M. Equations J and M have identical forms for this term ($v_q = \text{constant } \sigma_o d/L$), but the J value of the constant is exactly half the M value. The v_q term in equation S is dependent on $(f'_m)^{1/2}$. Figure 13, which plots the sum of the three terms, v_u , shows that no trends or similarities between equations can be easily identified from the single value of predicted ultimate strength.

The normalized plots (Figures 6 through 9) together with other data can be used to examine the stability or consistency of the predictive formulas. If two tests identical except in one parameter can be identified for which a predictive equation yields contradictory results, then the weight or even the functional form of that parameter in the formula becomes suspect. In the following paragraphs a selected number of cases are examined in this manner, placing emphasis on equations S and M, both of which were developed from masonry data and are proposed for use in masonry design.

Consider the stress ratios based on equations S and M which are plotted in Figures 6 and 7. Specimens 25 and 28 from data set M are identical in all parameters except ρ_h . The values of ρ_h are 0 and 0.00668, respectively. (Note that 0.00762 was the highest value of ρ_h included in the test specimens.) The test results for these two specimens, 2.18 and 2.04 MPa (316 and 296 psi), are nearly the same. However the strength predictions, approximately equivalent by either equation, are 1.4 MPa (200 psi) and 2.6 MPa (380 psi) for the two specimens, an underestimate in the first case and an overestimate in the second. The inconsistent predictions for specimens 25 and 28 imply that in some cases (e.g. high ρ_h) equations S and M can overestimate the effect of horizontal reinforcement on ultimate shear strength by a substantial amount.

Equations S and M desensitize the effect of horizontal reinforcement in different ways. In equation S, v_s is proportional to $(\rho_h f_{yh})$ times a factor, $(L - 2d' - s_h)/L$, which varies from 0.26 (test no. 36, $r = 2.25$) to 0.77 (test no. 29, $r = 0.90$). As r and s_h decrease, the factor increases toward unity. Conversely, the effect of horizontal reinforcement decreases with increasing r and s_h , and may conceivably become zero or negative. For instance, assume $r = 3$ and $s_h = h/3$ (i.e. three levels of horizontal bars). Then, $L = s_h$, resulting in a factor which is negative. The average value of the factor is 0.55 for the 62 tests. Equation M desensitizes the effect of horizontal reinforcement by using the expression $0.1575(\rho_h f_{yh} f'_m)^{1/2}$. Thus, as ρ_h increases, its effect on

strength increases at a decreasing rate. Both equations, however, tend to overestimate the effect of horizontal reinforcement on ultimate strength in more heavily reinforced walls.

Results for specimens from data set B provide additional information useful in identifying unsuccessful parametric forms. Consider the S-B comparison, as shown in Figure 6. Recall that the deviation of this set of predictions was relatively high, (0.64 MPa or 93 psi, Table 3). Specimens numbered 49, 51, 53, 55, 57 have identical axial load and are nearly identical in the other parameters. Equation S overestimates the ultimate strengths of these specimens by 11% to 38% (Figure 6). By comparison, equation M overestimates the strengths of the same specimens by -4% (underestimate) to 31% (Figure 7). Comparing averages, equations S and M overestimate the five tests by 27% and 11%, respectively. Recall that the M-B correlation shows considerably less scatter (Table 3) than predictions by other equations for this data set and that the deviation of the M-B comparison was 0.34 MPa (59 psi). The difference in the predictive accuracy of these two equations is mainly due to the differences in the effect of the v_s term on estimated strength. For these specimens, the range of differences in predictions for the v_m term was only from 0.14 to -0.18 MPa (20 to -26 psi). This difference was calculated as S prediction - M prediction. The difference in predicted effect of the v_s term (axial load) was only 0.19 MPa (27 psi). However the difference in the predicted contribution of horizontal steel strength to ultimate strength ranged from 0.50 to 0.96 MPa (72 to 139 psi). Equation S predicted values from 1.47 to 2.03 MPa (213 to 295 psi) for the horizontal steel strength term for these specimens, while equation M predicted contributions from 0.97 to 1.07 MPa (141 to 156 psi). This demonstrates that equation S gives excessive weight to the effect of horizontal steel on the ultimate strength of these specimens.

The predictions for the six double-wythe brick walls in data set B (specimen numbers 59-62) were also examined. The results from these specimens indicated that the effect of horizontal steel on ultimate strength is not accurately modeled by either equation. Equation S, and to a lesser extent equation M, underestimate the strengths of specimens 59, 61, and 62, which have low ρ_h (0.08 to 0.11%), and overestimate the strength of specimen 60, which has a high ρ_h (0.35%).

The above observations demonstrate that both equations S and M need to be examined with the aim of rendering predicted strength less sensitive to the horizontal reinforcement ratio.

6. CONCLUSIONS

The following conclusions can be drawn on the basis of the ultimate strength comparisons discussed above. Equation U does not adequately predict ultimate shear strength for the range of parameters represented by the masonry walls included in this study. Equation J is less consistent than equations S and M primarily because it gives excessive weight to the contribution of interior vertical bars in resisting shear forces. Equation S can predict shear strength well for only limited ranges of variables, primarily because it tends to overestimate the effect of horizontal reinforcement on strength. Of the four equations examined, equation M is generally the closest predictor of ultimate strength, but it lacks consistency. The parametric form of the horizontal steel ratio, ρ_h , has been identified as contributing to this inconsistency. The need to re-evaluate the effect of horizontal steel on strength (the v_s term) is indicated for both equations S and M. However, such re-evaluation cannot be carried out without a simultaneous re-evaluation of the weight given to v_m and v_q terms in contributing to predicted strength.

7. RECOMMENDATIONS

The experimental information compiled in this document and in other sources could be used to develop improved empirical relationships for closer and more consistent prediction of ultimate strength. The need for such improvements is underscored by the fact that the range of parameters encountered in actual masonry construction is wider than that of the test specimens examined in this study.

8. REFERENCES

1. Yancey, C.W.C., Fattal, S.G., Dikkers, R.D., Review of Technical Literature on Masonry Shear Walls, NISTIR 90-4512, National Institute of Standards and Technology, Gaithersburg, MD, December, 1990.
2. Shing, P.B., In-Plane Resistance of Reinforced Masonry Shear Walls, Fourth Meeting of U.S.-Japan Joint Technical Coordinating Committee on Masonry Research, San Diego, CA, October 1988.
3. Shing, P.B., Schuller, M., Hoskere, V.S., In-Plane Resistance of Masonry Shear Walls, Journal of Structural Engineering, ASCE, V116, No.3, March, 1990.
4. Matsumura, A., Shear Strength of Reinforced Hollow Unit Masonry Walls, Proceedings, 4th North American Masonry Conference, Paper No. 50, Los Angeles, CA, 1987.

5. Okamoto, S., Yamazaki, Y., Kaminosono, T., Teshigawara, M., and Hirashi, H., Seismic Capacity of Reinforced Masonry Walls and Beams, in Wind and Seismic Effects, Proceedings of the Eighteenth Joint Meeting, U.S.-Japan Panel on Wind and Seismic Effects, Raufaste, N.J., ed., NBSIR 87-3540, National Institute of Standards and Technology, Gaithersburg, MD, April, 1987.
6. Sveinsson, B.I., McNiven, H.D., and Sucuoglu, H., Cyclic Loading Tests of Masonry Single Piers, Vol. 4 - Additional Tests with Height to Width Ratio of 1, Report No. UCB/EERC-85-15, Earthquake Engineering Research Center, University of California, Berkeley, CA, December, 1985.
7. Uniform Building Code, 1988 Edition, International Conference of Building Officials, Whittier, CA, May 1, 1988.
8. Blume, John A., and Proulx, Jacques, Shear in Grouted Brick Masonry Wall Elements, Western States Clay Products Association, San Francisco, California, August 1968.
9. Blondet, J. Marcial, Mayes, Ronald A., Kelley, Trevor, Villablanca, Ricardo, F., and Klingner, Richard E., "Performance of Engineered Masonry in the Chilean Earthquake of March 3, 1985: Implications for U.S. Design Practice," Phil Ferguson Structural Engineering Laboratory, University of Texas, Austin, Texas, June 1989.
10. Leiva, Gilberto H., "Seismic Resistance of Two-Story Masonry Walls with Openings," PhD Dissertation, University of Texas, Austin, Texas, August, 1991.

APPENDIX A - Tables

TABLE A1. PROPERTIES OF SPECIMENS

TEST NUMBER	SPECIMEN LABEL	h in	L in	t in	d in	sh in	r	rd psi	f'm psi	fyh psi
1	3-S	72.00	72.00	5.625	68.00	16.00	1.00	1.06	3000	56000
2	4-S	72.00	72.00	5.625	68.00	16.00	1.00	1.06	2800	56000
3	5-S	72.00	72.00	5.625	68.00	16.00	1.00	1.06	2600	56000
4	7-S	72.00	72.00	5.625	68.00	16.00	1.00	1.06	3000	56000
5	8-S	72.00	72.00	5.625	68.00	16.00	1.00	1.06	3000	56000
6	13-S	72.00	72.00	5.625	68.00	16.00	1.00	1.06	3300	67000
7	14-S	72.00	72.00	5.625	68.00	16.00	1.00	1.06	3300	56000
8	16-S	72.00	72.00	5.625	68.00	16.00	1.00	1.06	2500	67000
9	21-S	72.00	72.00	5.375	68.00	16.00	1.00	1.06	3800	56000
10	22-S	72.00	72.00	5.375	68.00	16.00	1.00	1.06	3800	56000
11	KW4-1-M	70.87	62.60	5.906	59.06	15.75	1.13	1.20	3164	55878
12	KW3-1-M	70.87	46.85	5.906	43.31	15.75	1.51	1.64	3164	55878
13	KW3S-1-	70.87	46.85	5.906	43.31	15.75	1.51	1.64	3164	55878
14	KW2-1-M	70.87	31.10	5.906	27.58	15.75	2.28	2.57	3164	55878
15	WS2-M	70.87	46.85	7.480	43.11	15.75	1.51	1.64	3237	55878
16	WS4-M	70.87	46.85	7.480	43.11	15.75	1.51	1.64	3237	55878
17	WS5-M	70.87	46.85	7.480	43.11	15.75	1.51	1.64	3237	55878
18	WS9-M	70.87	46.85	7.480	43.11	15.75	1.51	1.64	3237	55878
19	WS10-M	70.87	46.85	7.480	43.11	15.75	1.51	1.64	3237	55878
20	WS9-2-M	70.87	46.85	7.480	43.11	15.75	1.51	1.64	4209	55878
21	WSB21-M	70.87	46.85	7.480	43.11	15.75	1.51	1.64	3788	55878
22	WSB22-M	70.87	46.85	7.480	43.11	15.75	1.51	1.64	3977	55878
23	WSB3-M	70.87	46.85	7.480	43.11	15.75	1.51	1.64	3832	55878
24	WSB4-M	70.87	46.85	7.480	43.11	15.75	1.51	1.64	4557	55878
25	WSR2-M	66.93	43.70	7.480	39.57	14.87	1.53	1.69	4151	55878
26	WSR4-M	66.93	43.70	7.480	39.57	14.87	1.53	1.69	4151	55878
27	WSR5-M	66.93	43.70	7.480	39.57	14.87	1.53	1.69	4151	55878
28	WSR6-M	66.93	43.70	7.480	39.57	14.87	1.53	1.69	4151	55878
29	WS1-O	70.87	78.74	7.480	75.00	15.75	0.90	0.94	2600	51442
30	WS4-O	70.87	47.24	7.480	43.50	15.75	1.50	1.63	3311	51442
31	WS7-O	70.87	31.50	7.480	27.76	15.75	2.25	2.55	2600	51442
32	WSN1-O	70.87	47.24	7.480	43.50	15.75	1.50	1.63	3311	51442
33	WSN2-O	70.87	47.24	7.480	43.50	15.75	1.50	1.63	3311	51442
34	WSR1-O	70.87	78.74	7.480	75.00	15.75	0.90	0.94	3879	51442
35	WSR4-O	70.87	47.24	7.480	43.50	15.75	1.50	1.63	3652	51442
36	WSR7-O	70.87	31.50	7.480	27.76	15.75	2.25	2.55	3098	51442
37	WSRC-O	70.87	47.24	7.480	43.50	15.75	1.50	1.63	3879	51442
38	CB13-B	56.00	48.00	5.625	45.00	11.20	1.17	1.24	3359	59000
39	CB15-B	56.00	48.00	5.625	45.00	11.20	1.17	1.24	3359	59000
40	CB17-B	56.00	48.00	5.625	45.00	11.20	1.17	1.24	2297	63500
41	CB18-B	56.00	48.00	5.625	45.00	11.20	1.17	1.24	2297	63500
42	CB20-B	56.00	48.00	5.625	45.00	18.67	1.17	1.24	2196	63500
43	CB21-B	56.00	48.00	5.625	45.00	18.67	1.17	1.24	2196	63500
44	CB23-B	56.00	48.00	5.625	45.00	8.00	1.17	1.24	2196	63500
45	CB24-B	56.00	48.00	5.625	45.00	15.72	1.17	1.24	2196	63500
46	CB25-B	56.00	48.00	5.625	45.00	18.67	1.17	1.24	2196	63500
47	CB26-B	56.00	48.00	5.625	45.00	18.67	1.17	1.24	2196	63500
48	BR19-B	56.00	48.00	5.625	45.00	18.67	1.17	1.24	2918	63500
49	BR20-B	56.00	48.00	5.625	45.00	9.33	1.17	1.24	2918	63500
50	BR21-B	56.00	48.00	5.625	45.00	18.67	1.17	1.24	2918	63500
51	BR22-B	56.00	48.00	5.625	45.00	9.33	1.17	1.24	2918	63500
52	BR23-B	56.00	48.00	5.625	45.00	18.67	1.17	1.24	2918	63500
53	BR24-B	56.00	48.00	5.625	45.00	9.33	1.17	1.24	2918	63500
54	BR25-B	56.00	48.00	5.625	45.00	18.67	1.17	1.24	2918	63500
55	BR26-B	56.00	48.00	5.625	45.00	9.33	1.17	1.24	2918	63500
56	BR27-B	56.00	48.00	5.625	45.00	11.20	1.17	1.24	2918	59500
57	BR28-B	56.00	48.00	5.625	45.00	5.08	1.17	1.24	2918	60500
58	BR30-B	56.00	48.00	5.625	45.00	8.00	1.17	1.24	4008	63500
59	DBR8-B	56.00	48.00	10.000	45.00	28.00	1.17	1.24	2483	59000
60	DBR9-B	56.00	48.00	10.000	45.00	9.33	1.17	1.24	2483	67500
61	DBR10-B	56.00	48.00	10.000	45.00	28.00	1.17	1.24	2483	59000
62	DBR12-B	56.00	48.00	10.000	45.00	15.17	1.17	1.24	2483	57800

TABLE A1 CONT'D PROPERTIES OF SPECIMENS

TEST NUMBER	SPECIME LABEL	fyve psi	fyvi psi	fyv psi	ph	pve	pvi psi	pv	SIGMAO psi	ALPHA
1	3-S	72000	72000	72000	0.00122	0.00148	0.00667	0.00741	0	1
2	4-S	72000	72000	72000	0.00122	0.00148	0.00667	0.00741	0	1
3	5-S	72000	72000	72000	0.00122	0.00148	0.00667	0.00741	0	1
4	7-S	72000	72000	72000	0.00122	0.00148	0.00667	0.00741	0	1
5	9-S	64000	64000	64000	0.00122	0.00077	0.00344	0.00383	0	1
6	13-S	65000	65000	65000	0.00222	0.00109	0.00489	0.00543	0	1
7	14-S	65000	65000	65000	0.00122	0.00109	0.00489	0.00543	0	1
8	16-S	72000	72000	72000	0.00222	0.00148	0.00667	0.00741	0	1
9	21-S	65000	65000	65000	0.00128	0.00114	0.00512	0.00568	0	1
10	22-S	65000	65000	65000	0.00128	0.00114	0.00512	0.00568	0	1
11	KW4-1-M	55878	55878	55878	0.00118	0.00426	0.00134	0.00943	0	0.5
12	KW3-1-M	55878	55878	55878	0.00118	0.00434	0.00140	0.00946	0	0.5
13	KW3S-1-	55878	55878	55878	0.00118	0.00434	0.00140	0.00946	0	0.5
14	KW2-1-M	55878	55878	55878	0.00118	0.00541	0.00155	0.01148	0	0.5
15	WS2-M	55878	55878	55878	0.00000	0.00254	0.00111	0.00571	0	0.5
16	WS4-M	55878	55878	55878	0.00167	0.00254	0.00111	0.00571	0	0.5
17	WS5-M	55878	55878	55878	0.00334	0.00254	0.00111	0.00571	0	0.5
18	WS9-M	55878	55878	55878	0.00334	0.00448	0.00111	0.00959	0	0.5
19	WS10-M	55878	55878	55878	0.00668	0.00448	0.00111	0.00959	0	0.5
20	WS9-2-M	55878	55878	55878	0.00334	0.00448	0.00111	0.00959	0	0.5
21	WSB21-	55878	55878	55878	0.00334	0.00448	0.00111	0.00959	0	0.5
22	WSB22-	55878	55878	55878	0.00400	0.00448	0.00111	0.00959	0	0.5
23	WSB3-M	55878	55878	55878	0.00353	0.00473	0.00117	0.01013	0	0.5
24	WSB4-M	55878	55878	55878	0.00334	0.00448	0.00111	0.00959	0	0.5
25	WSR2-M	55878	55878	55878	0.00000	0.00272	0.00121	0.00812	0	0.5
26	WSR4-M	55878	55878	55878	0.00167	0.00272	0.00121	0.00812	0	0.5
27	WSR5-M	55878	55878	55878	0.00334	0.00272	0.00121	0.00812	0	0.5
28	WSR6-M	55878	55878	55878	0.00668	0.00272	0.00121	0.00812	0	0.5
29	WS1-O	56103	53872	54987	0.00167	0.00149	0.00292	0.00509	0	0.5
30	WS4-O	56103	53872	54987	0.00167	0.00249	0.00316	0.00674	0	0.5
31	WS7-O	56103	53872	54987	0.00167	0.00374	0.00351	0.00879	0	0.5
32	WSN1-O	56103	53872	54987	0.00167	0.00249	0.00316	0.00674	0	0.5
33	WSN2-O	56103	53872	54987	0.00167	0.00249	0.00316	0.00674	0	0.5
34	WSR1-O	56103	52693	54398	0.00167	0.00149	0.00292	0.00509	0	0.5
35	WSR4-O	56103	53872	54987	0.00167	0.00249	0.00316	0.00674	0	0.5
36	WSR7-O	56103	53872	54987	0.00167	0.00374	0.00351	0.00879	0	0.5
37	WSRC-O	56103	53872	54987	0.00167	0.00249	0.00316	0.00674	0	0.5
38	CB13-B	67500	67500	67500	0.00281	0.00085	0.00000	0.00169	0	0.5
39	CB15-B	67500	67500	67500	0.00281	0.00085	0.00000	0.00169	0	0.5
40	CB17-B	56700	56700	56700	0.00394	0.00222	0.00000	0.00444	0	0.5
41	CB18-B	59500	59500	59500	0.00394	0.00074	0.00423	0.00444	0	0.5
42	CB20-B	56700	56700	56700	0.00197	0.00222	0.00000	0.00444	0	0.5
43	CB21-B	59500	59500	59500	0.00197	0.00074	0.00423	0.00444	0	0.5
44	CB23-B	56700	56700	56700	0.00075	0.00222	0.00000	0.00444	0	0.5
45	CB24-B	56700	56700	56700	0.00272	0.00222	0.00000	0.00444	0	0.5
46	CB25-B	56700	56700	56700	0.00197	0.00222	0.00000	0.00444	0	0.5
47	CB26-B	56700	56700	56700	0.00197	0.00222	0.00000	0.00444	0	0.5
48	BR19-B	56700	56700	56700	0.00197	0.00222	0.00000	0.00444	0	0.5
49	BR20-B	56700	56700	56700	0.00492	0.00222	0.00000	0.00444	0	0.5
50	BR21-B	56700	56700	56700	0.00197	0.00222	0.00394	0.00674	0	0.5
51	BR22-B	63500	63500	63500	0.00492	0.00115	0.00394	0.00459	0	0.5
52	BR23-B	59500	59500	59500	0.00197	0.00074	0.00423	0.00444	0	0.5
53	BR24-B	59500	59500	59500	0.00492	0.00074	0.00423	0.00444	0	0.5
54	BR25-B	56700	56700	56700	0.00197	0.00222	0.00000	0.00148	0	0.5
55	BR26-B	56700	56700	56700	0.00492	0.00222	0.00000	0.00444	0	0.5
56	BR27-B	56700	56700	56700	0.00254	0.00222	0.00000	0.00444	0	0.5
57	BR28-B	59500	59500	59500	0.00635	0.00222	0.00000	0.00444	0	0.5
58	BR30-B	56700	56700	56700	0.00100	0.00222	0.00000	0.00444	0	0.5
59	DBR8S-B	67500	67500	67500	0.00055	0.00065	0.00000	0.00129	0	0.5
60	DBR9-B	67500	67500	67500	0.00277	0.00065	0.00000	0.00129	0	0.5
61	DBR10-B	67500	67500	67500	0.00055	0.00065	0.00000	0.00129	0	0.5
62	DBR12-B	67500	67500	67500	0.00059	0.00065	0.00000	0.00129	0	0.5

TABLE A2. PREDICTIONS AND TEST RESULTS

TEST NUMBER	SPECIMEN LABEL	**** Vm psi **				**** Vs psi *				**** Vq psi *				**** Vu = Vm+Vs + Vq**				Vu TEST psi
		S	M	J	U	S	M	J	U	S	M	J	U	S	M	J	U	
1	3-S	162	158	49	68	46	40	254	68	27	45	22	0	234	243	325	134	253
2	4-S	151	147	45	61	46	38	254	68	0	0	0	0	197	185	299	130	196
3	5-S	151	147	45	61	46	38	254	68	9	17	8	0	206	202	307	130	214
4	7-S	162	158	49	66	46	40	254	68	10	17	8	0	218	215	311	134	240
5	9-S	134	130	42	66	46	40	194	68	27	45	22	0	206	215	259	134	237
6	13-S	151	151	48	69	99	63	253	149	28	45	22	0	279	259	323	218	278
7	14-S	151	151	48	69	46	42	220	68	28	45	22	0	225	238	290	137	259
8	16-S	148	145	44	60	99	54	287	149	24	45	22	0	272	244	353	209	298
9	21-S	164	165	52	74	48	47	225	72	31	46	23	0	243	258	300	146	260
10	22-S	164	165	52	74	48	47	225	72	11	17	8	0	223	228	285	146	226
11	KW4-1-M	166	207	64	103	42	68	141	66	7	12	6	0	215	287	211	169	232
12	KW3-1-M	166	167	63	84	34	66	140	66	7	12	6	0	207	245	208	150	250
13	KW3S-1-	166	167	63	84	34	66	140	66	7	12	6	0	207	245	208	150	271
14	KW2-1-M	177	124	56	67	18	64	138	66	7	11	6	0	202	199	199	133	234
15	WS2-M	146	143	56	84	0	0	65	0	29	48	23	0	176	189	143	84	247
16	WS4-M	146	143	56	84	47	80	144	93	29	48	23	0	223	268	222	178	274
17	WS5-M	146	143	56	84	94	113	176	187	29	46	23	0	270	301	255	271	331
18	WS9-M	169	169	64	84	94	113	176	187	29	48	23	0	292	328	263	271	332
19	WS10-M	169	169	64	84	188	159	223	373	29	46	23	0	386	374	309	458	425
20	WS9-2-M	192	193	74	96	94	128	178	187	33	46	23	0	320	367	274	283	376
21	WSB21-M	182	183	70	91	94	122	176	187	32	46	23	0	308	351	269	278	325
22	WSB22-M	187	188	72	94	113	137	187	224	32	46	23	0	332	370	282	317	382
23	WSB3-M	187	187	71	92	99	126	181	197	32	48	23	0	318	359	275	289	353
24	WSB4-M	200	201	78	100	94	134	176	187	35	48	23	0	329	380	278	287	378
25	WSR2-M	169	159	65	93	0	0	66	0	33	45	23	0	201	204	153	93	316
26	WSR4-M	169	159	65	93	44	89	144	93	33	45	23	0	245	293	231	187	283
27	WSR5-M	169	159	65	93	88	126	176	187	33	45	23	0	289	330	264	280	248
28	WSR6-M	169	159	65	93	176	178	222	373	33	45	23	0	377	382	309	466	296
29	WS1-O	128	159	46	104	61	71	185	86	0	0	0	0	188	230	231	190	388
30	WS4-O	153	144	56	86	44	77	183	86	29	48	23	0	227	268	262	172	285
31	WS7-O	146	100	47	61	23	66	181	86	0	0	0	0	169	166	228	147	296
32	WSN1-O	153	144	56	86	44	77	183	86	59	92	46	0	256	313	285	172	349
33	WSN2-O	153	144	56	86	44	77	183	86	88	137	69	0	285	359	308	172	379
34	WSR1-O	156	194	57	127	61	87	184	86	0	0	0	0	216	281	241	213	453
35	WSR4-O	181	152	60	90	44	81	183	86	0	0	0	0	205	233	243	176	338
36	WSR7-O	180	110	51	67	23	72	181	86	0	0	0	0	182	181	232	153	296
37	WSRC-O	166	156	62	93	44	84	183	86	35	50	25	0	245	291	270	179	317
38	CB13-B	128	128	45	105	106	110	108	166	28	45	22	0	263	283	175	270	283
39	CB16-B	128	128	45	105	106	110	108	166	46	72	36	0	280	310	189	270	345
40	CB17-B	118	141	46	86	160	112	132	250	35	66	33	0	312	318	211	336	357
41	CB18-B	119	101	36	86	160	112	265	250	35	66	33	0	314	279	333	336	357
42	CB20-B	115	138	45	85	61	77	93	125	34	66	33	0	209	281	171	210	342
43	CB21-B	116	99	35	85	61	77	226	125	34	66	33	0	211	242	294	210	324
44	CB23-B	115	138	45	85	34	48	58	48	34	66	33	0	182	251	136	132	278
45	CB24-B	115	138	45	85	94	91	110	173	34	66	33	0	243	294	188	257	353
46	CB25-B	115	138	45	85	61	77	93	125	21	41	21	0	197	257	159	210	285
47	CB26-B	115	138	45	85	61	77	93	125	34	66	33	0	209	281	171	210	349
48	BR19-B	133	159	52	97	61	89	93	125	39	66	33	0	232	314	178	222	267
49	BR20-B	133	159	52	97	213	141	148	312	39	66	33	0	384	365	233	410	278
50	BR21-B	145	159	52	97	61	89	218	125	39	66	33	0	245	314	303	222	341
51	BR22-B	136	130	45	97	213	141	280	312	39	66	33	0	388	337	357	410	348
52	BR23-B	134	114	41	97	61	89	226	125	39	66	33	0	233	269	299	222	295
53	BR24-B	134	114	41	97	213	141	280	312	39	66	33	0	385	321	353	410	320
54	BR25-B	116	159	52	97	61	89	93	125	39	66	33	0	216	314	178	222	316
55	BR26-B	133	159	52	97	213	141	148	312	39	66	33	0	384	365	233	410	311
56	BR27-B	133	159	52	97	97	98	103	151	39	66	33	0	268	323	188	249	327
57	BR28-B	134	159	52	97	285	156	164	384	39	66	33	0	468	381	249	482	330
58	BR30-B	155	186	63	114	45	74	67	64	46	66	33	0	248	326	162	178	391
59	DBR8S-B	107	101	36	90	10	42	48	33	20	36	18	0	137	179	102	123	216
60	DBR9-B	107	101	36	90	127	101	114	187	30	55	27	0	264	256	178	277	237
61	DBR10-B	107	101	36	90	10	42	48	33	30	55	27	0	147	196	111	123	251
62	DBR12-B	0	0	0	0	0	0	0	0	0	0	0	0	0	0	0	0	0

Table A3 - Deviation (s), Mean (x), and Variation (v) in predicted vs test strengths (psi)

DATA SET	STATS	EQUATION			
		S	M	J	U
S	s	21.19	23.95	67.63	101.74
	x	246.01	246.01	246.01	246.01
	v	0.09	0.10	0.28	0.41
M	s	56.46	48.19	81.71	108.13
	x	308.42	308.42	308.42	308.42
	v	0.18	0.18	0.27	0.35
O	s	145.14	145.14	111.32	183.89
	x	344.41	344.41	344.41	344.41
	v	0.42	0.42	0.32	0.53
B	s	93.32	93.32	122.64	109.14
	x	311.03	311.03	311.03	311.03
	v	0.30	0.16	0.39	0.35
TOTAL	s	84.47	57.62	100.44	118.00
	x	304.64	304.64	304.64	304.64
	v	0.28	0.19	0.33	0.39

APPENDIX B - Derivations

The original forms of the equations studied in this report are presented here, with explanations of the reformulations required to achieve common format and consistent units.

Equation S

Proposed equations (15) and (16) in Reference [3] by Shing et al. were combined to form equation S which was examined in this study. The original equations are:

$$\begin{aligned}V_n &= V_m + V_s \\V_m &= [0.0018 (\rho_v f_y + \sigma_c) + 2] A \sqrt{f'_m} \\V_s &= \left[\frac{L - 2d'}{s - 1} \right] A_h f_y\end{aligned}$$

(15)

(16)

The notation was changed to the common forms defined in section 3.3 of this paper, by introducing symbols f_{yv} and f_{yh} for the yield strengths of vertical and horizontal steel in lieu of f_y in the original equations. The notations s and σ_c were changed to s_h and σ_o , respectively. The other symbols are unchanged.

The equations were transformed from force to stress units by dividing by the gross area, A . The two terms of equation (15) above become the first and third terms of equation S after conversion from U.S. Customary units to SI units. After division by A , equation (16) above becomes the second term of equation S. Equation S as introduced in section 3.2 accounts for the conversion from U.S. Customary units to SI units. Note that $A_h/A = s_h \rho_h/L$.

Equation M

Matsumura proposed a formula for predicting ultimate shear force on a masonry shear wall in Reference [4]. This equation, numbered (5) in the reference, is:

$$V_u = [k_u k_p \left(\frac{0.76}{\frac{h}{d} + 0.7} + 0.012 \right) \sqrt{f'_{m(g)}} + (0.18 \gamma \sigma \sqrt{P_H H \sigma_y f'_{m(g)}} + 0.2 \sigma_{o(g)})] 10^3 t j \quad (5)$$

In this equation, $k_p = 1.16 \rho_t^{0.3}$. For brick and fully grouted concrete block masonry walls coefficients k_u and γ are equal to 1.0 and are eliminated from the equation. In accordance with the definitions in section 3.3, the notation is changed as follows:

$$\rho_t = \rho_{ve}; f'_{m(g)} = f'_m; P_H = P_h; H \sigma_y = f_{yh}; \sigma_{o(g)} = \sigma_o; j = 0.875 d'; (h/d) = r_d$$

After division of both sides by gross area (tL), the three terms of equation (5) above become the three terms of equation M.

Equation J

The original form of equation J is given by equation (1) of reference [5], which cites the Reinforced Concrete Standards of the Architectural Institute of Japan as the source of the equation:

$$\tau_{SH} = \left[\frac{0.053 P_{te}^{0.23} (f'_m + 180)}{\left(\frac{M}{QD} \right) + 0.12} + 2.7 \sqrt{\sigma_{wh} P_{we}} + 0.1 \sigma_{oe} \right] \frac{B_e j}{BD} \quad (1)$$

The notation is changed in accordance with the notation of section 3.3 as follows:

$$P_{te} = \rho_{ve}; D = L; \sigma_{oe} = \sigma_o; B_e = B = t$$

where M/QD is bounded as follows: $1 \leq M/QD \leq 3$

The notation is changed in accordance with the notation of section 3.3 as follows:

$$P_{te} = \rho_{ve}; D = L; \sigma_{oe} = \sigma_o; B_e = B = t; M/QD = r_c$$

However, since M/QD is discontinuous, r_c is expressed as a discontinuous function of αr to satisfy the bounds on M/QD ,

$$r_c = 1 + \langle \alpha r - 1 \rangle - \langle \alpha r - 3 \rangle$$

where for any real number, $\langle a \rangle = 0$ for $a \leq 0$ and $\langle a \rangle = a$ for $a > 0$. Note that for cantilever walls (test series S), $M/QD = h/L = r$ ($\alpha = 1$), and for walls with the top and bottom rotationally fixed (test series M, O, and B), $M/QD = h/2L = r/2$ ($\alpha = 1/2$).

In the term $2.7(\sigma_{wh}P_{we})^{1/2}$, σ_{wh} is the yield strength of shear reinforcement (kg/cm²) and P_{we} is the ratio of shear reinforcement. Both horizontal reinforcement and interior vertical bars are treated as shear reinforcement (vertical bars in the two exterior cores are excluded). Accordingly, the second term in the above equation is separated into the sum of two terms to distinguish between horizontal and vertical shear reinforcement and their respective shear strengths. After conversion to the notation adopted in this report, the second term becomes:

$$2.7\sqrt{\sigma_{wh}P_{we}} = 2.7\sqrt{\rho_{yh}f_{yh}} + 2.7\sqrt{\rho_{yvi}f_{yvi}}$$

which, after conversion from the cgs system to U.S. Customary Units, becomes identical to the second term of equation J.

Substituting $0.875d$ for j , the first and third terms of equation (1) above become the first and third terms of equation J after conversion to SI units is made.

Equation U

The original form of equation U is given by combining equations (12-13), (12-14), and (12-15) of the 1988 Uniform Building Code [7].

$$V_n = V_m + V_s \quad (12-13)$$

$$V_m = C_d A_{mv} \sqrt{f'_m} \quad (12-14)$$

$$V_s = A_{mv} \rho_n f_y \quad (12-15)$$

The notation is changed to conform with the notation in section 3.3 as follows:

$$A_{mv} = A; \rho_n = \rho_h; f_y = f_{yh}; V_n = V_u$$

C_d in the above equation is a discontinuous function of $M/V_u d$,

$$C_d = 2.4 \text{ for } (M/Vd) \leq 0.25$$

$$C_d = 1.2 \text{ for } (M/Vd) \geq 1.00$$

or expressed in functional form,

$$C_d = 2.4 + 1.6 \langle ar_d - 1 \rangle - 1.6 \langle ar_d - 0.25 \rangle$$

The numerical coefficient 0.083 in the first term of equation U is obtained by conversion of the UBC equation (12 - 14) to SI units. Note that the UBC equations do not consider axial load to contribute to strength, thus there is no third term in equation U.